Identification of Nonlinear Wave Forces. Part I: Time-Domain Analysis

K Worden, P K Stansby and G R Tomlinson
Department of Engineering
University of Manchester
Oxford Road
Manchester
M13 9PL

S A Billings
Department of Automatic Control and Systems Engineering
University of Sheffield
P O Box 600
Mappin Street
Sheffield
S1 4DU

Research Report No 441

October 1991

Identification of Nonlinear Wave Forces. Part I: Time-Domain Analysis.

K.Worden, P.K.Stansby and G.R.Tomlinson
Department of Engineering
The University
Oxford Road
Manchester M13 9PL

S.A.Billings
Department of Automatic Control and Systems Engineering
University of Sheffield
Mappin Street
Sheffield S1 3JD

Abstract

The NARMAX system identification technique is applied to a number of fluid loading data sets in order to determine if there exists a simple extension of Morison's equation which will predict forces with improved accuracy. Data from a variety of flow situations is considered, ranging from regular planar oscillatory flow in a U-tube, to unidirectional irregular waves in a wave flume, to directional seas in Christchurch Bay.

1 Introduction

Since its introduction in 1950 [1], the Morison equation has provided the main means of predicting wave forces on slender cylinders. In the usual notation,

$$F(t) = \frac{1}{2}\rho D C_d u|u| + \frac{1}{4}\pi\rho D^2 C_m \dot{u} \tag{1}$$

where $F(t)$ is the force per unit axial length, $u(t)$ is the instantaneous flow velocity, ρ is water density and D is diameter. The dimensionless drag and inertia coefficients C_d and C_m depend on the characteristics of the flow. In general the main dependence is taken to be on Re, the Reynolds number, and KC, the Keulegan-Carpenter number although these parameters do not have generally accepted definitions in random or directional waves. In place of Re, the Stokes parameter $\beta = Re/KC$ is often used.

The coefficients C_d and C_m are usually obtained by applying least-squares procedures to measured force and velocity data.

The equation generally predicts the main trends in measured data quite well; however, some characteristics of the flow are not well represented. For example, in sinusoidal oscillatory flow the force variation at the fundamental frequency may be well predicted while that at higher harmonics is not. One result is that peak forces can be underpredicted. Further, a poor representation of the high frequency content of the forces is a serious limitation for the determination of the fatigue life of a structural element.

The publication [2] documented an attempt to determine new model structures on heuristic physical grounds. It was found that two simple extended equations allowed a considerable increase in the accuracy of curve-fits to data measured in a variety of flow situations, ranging from sinusoidal flow in a U-tube, to unidirectional random waves in a large wave flume, to directional seas in Christchurch Bay. The first of these new structures simply extended the Morison equation through the addition of a term in $F|F|$. The addition of this single term allowed a finer classification of wave forces due to the fact that a significant contribution from the extra term was found to be correlated with the presence of gross vortex shedding effects. The second of the new structures also included derivatives of the force $\dot{F}$ and $\ddot{F}$, yielding a variant of Duffing's equation for a nonlinear oscillator - the Morison/Duffing equation. Although the adoption of these new structures resulted in improved curve fits, predictions of the fluid forces were disappointing. (The important distinction between curve-fit accuracy and prediction accuracy as measures of model validity is discussed in detail in Section 4 below.) The approach taken here is to allow sophisticated system identification techniques based on NARMAX models [4] free rein in deciding the appropriate terms for an extended model in an attempt to produce good fits and predictions. The extra terms produced may have no obvious relation to the flow phenomena involved. Previous work of this kind has been limited to the addition of velocity-based terms with applications to U-tube data [3].

The layout of the paper is as follows: Section 2 provides an introduction to system identification using the NARMAX nonlinear time series analysis procedures. Section 3 provides a summary of the basic theory required for any parameter estimation problem; also the problem of ***structure detection*** i.e. determining the appropriate form for the system model is discussed. Section 4 deals with the subject of model validation. In Section 5, a simulation of a Morison-type system is used to demonstrate the utility of the NARMAX procedures in analysing fluid loading data. Section 6 describes the results of applying the techniques to experimental data measured in a U-tube. Section 7 progresses to a discussion of unidirectional random waves in a large flume. Finally, data from a directional random sea measured at the Christchurch Bay tower is discussed in Section 8.

Throughout this study, all the analysis is carried out in the time-domain. Part II of this paper [6] will contain a description of the parallel results obtained in the frequency-domain.

2 System Identification via NARMAX Modelling.

Although almost all of the methodology presented here is documented elsewhere in the literature [7] [8] [9] [4] [10] [11], it is likely that it is unfamiliar within the context of fluid loading problems. For this reason a discussion is included here for the sake of completeness.

The basic object of system identification can be stated quite simply. Given a physical system which reponds in some measurable way $y_s(t)$ when an external stimulus or excitation $x(t)$ is applied, one wishes to determine a mathematical model of the system which responds with an identical output $y_m(t)$ when given the same stimulus. The model will generally be some functional which maps the input $x(t)$ to the output $y_m(t)$.

$$y_m(t) = S[x](t) \tag{2}$$

If the model changes when the frequency or amplitude characteristics of the excitation changes, it is said to be ***input-dependent***. Such models are unsatisfactory in that they may have very limited predictive capabilities.

The problem of system identification is to obtain an appropriate functional S for a given system. If *a priori* information about the system is available, the complexity of the problem can be reduced considerably; for example, suppose that the system is known to be a linear single degree-of-freedom dynamical system. In this case the form of the equation relating $x(t)$ and $y(t)$ is known to be

$$m\ddot{y} + c\dot{y} + ky = x(t) \tag{3}$$

where overdots denote differentiation with respect to time. In this case the only unknowns are the coefficients or parameters m, c, and k; the problem has been reduced to one of *parameter estimation*. Alternatively, rewriting equation (3) as

$$(Ly)(t) = x(t) \tag{4}$$

where L is a second order linear differential operator, one can write the solution as

$$y(t) = (L^{-1}x)(t) = \int d\tau h(\tau - t)x(\tau) \tag{5}$$

which explicitly displays $y(t)$ as a *linear* functional of $x(t)$. Within this framework, the system is identified by obtaining a representation of the function $h(t)$ which is often referred to as the impulse response or Green's function for the system. In structural dynamics $h(t)$ is usually obtained via its Fourier transform $H(\omega)$ which is the system transfer function

$$H(\omega) = \frac{Y(\omega)}{X(\omega)} \tag{6}$$

where $X(\omega)$ and $Y(\omega)$ are the Fourier transforms of $x(t)$ and $y(t)$ respectively. It is a simple matter to show that the transfer function for the system (3) has the form

$$H(\omega) = \frac{1}{-m\omega^2 + ic\omega + k} \tag{7}$$

and $H(\omega)$ is completely determined by the three parameters m,c and k as expected. This example shows the striking duality between the time and frequency domain representations for a linear system. In fact, this duality extends naturally to nonlinear systems where the analogues of both the impulse response and transfer functions can be defined. This representation of nonlinear systems will be discussed in considerable detail in the second part of this study [6].

A discussion of the mathematical details of the parameter estimation algorithm is deferred until the following section. The main requirement is that measured time data should be available for each term in the model equation which has been assigned

a parameter. In the case of equation (3), one would need records of displacement $y(t)$, velocity $\dot{y}(t)$, acceleration $\ddot{y}(t)$ and force $x(t)$ in order to estimate the parameters. A simpler approach is to adopt a discrete-time representation of equation (3). If the input and output signals are sampled at regular intervals of time Δt, one obtains records of data $x_i = x(i\Delta t)$ and $y_i = y(i\Delta t)$ for $i = 1, \ldots, N$ related by

$$m\ddot{y}_i + c\dot{y}_i + ky_i = x_i \tag{8}$$

The velocity and acceleration can be approximated by difference formulae

$$\dot{y}_i = \frac{y_i - y_{i-1}}{\Delta t} \tag{9}$$

$$\ddot{y}_i = \frac{y_{i+1} - 2y_i + y_{i-1}}{\Delta t^2} \tag{10}$$

Substituting these expressions into (8) gives

$$y_i = \left\{2 - \frac{c\Delta t}{m} - \frac{k\Delta t^2}{m}\right\} y_{i-1} + \left\{\frac{c\Delta t}{m} - 1\right\} y_{i-2} + \frac{\Delta t^2}{m} x_{i-1} \tag{11}$$

or

$$y_i = a_1 y_{i-1} + a_2 y_{i-2} + b_1 x_{i-1} \tag{12}$$

This linear difference equation is one of the possible discrete-time representations of the system in equation (3), the fact that it is not unique is a consequence of the fact that there are many different discrete representations of derivatives. As a result, the discrete form (12) will provide a representation which is as accurate as the approximations (9) and (10). A further level of non-uniqueness is reflected in the fact that the parameters depend on the sampling interval Δt. In the time-series literature this type of model is termed Auto-Regressive with eXogenous inputs (ARX). The words 'auto-regressive' refer to the fact that the present output value is partly determined by or regressed on, previous output values. The regression on past input values is indicated by the words 'exogenous inputs' (the term exogenous arose originally in the literature of econometrics).

Through the discretisation process, the input-output functional of equation (2) has become a linear input-output function with the form

$$y_i = F(y_{i-1}, y_{i-2}; x_{i-2}) \tag{13}$$

The advantage of adopting this form is that only the two states x and y need be measured in order to estimate all the model parameters a_1,a_2 and b_1 in (12) and thus identify the system. It is a simple matter to show that a general linear system has a discrete-time representation

$$y_i = \sum_{j=1}^{n_y} a_j y_{i-j} + \sum_{j=1}^{n_x} b_j x_{i-j} \tag{14}$$

or

$$y_i = F(y_{i-1}, \ldots, y_{i-n_y}; x_{i-1}, \ldots, x_{i-n_x}) \tag{15}$$

As before, all parameters $a_1, \ldots, a_{n_y}, b_1, \ldots, b_{n_x}$ can be estimated using measurements of the x and y data only.

The extension to nonlinear systems is straightforward. Consider the Duffing oscillator represented by

$$m\ddot{y} + c\dot{y} + ky + k_3y^3 = x(t) \tag{16}$$

This continuous-time system is identified by estimating the parameters m, c, k and k_3. Alternatively, one can pass to the discrete-time representation

$$y_i = a_1y_{i-1} + a_2y_{i-2} + b_1x_{i-1} + cy_{i-1}^3 \tag{17}$$

where a_1,a_2 and b_1 are unchanged from (11) and

$$c = \frac{\Delta t^2 k_3}{m} \tag{18}$$

The model (17) is now termed a NARX (Nonlinear ARX) model. The regression function $y_i = F(y_{i-1}, y_{i-2}; x_{i-2})$ is now nonlinear; it contains a cubic term. If *all* terms of order three or less were included in the model structure i.e. $(y_{i-2})^2x_{i-1}$ etc. a much more general model would be obtained,

$$y_i = F^{(3)}(y_{i-1}, y_{i-2}; x_{i-2}) \tag{19}$$

(the superscript denotes the highest order product terms) which would be sufficiently general to represent the behaviour of any dynamical systems with nonlinearities up to third order i.e. containing terms of the form $\dot{y}^3$, $\dot{y}^2y$ etc.

The most general polynomial NARX model (including products of order $\leq n_p$) is denoted by

$$y_i = F^{(n_p)}(y_{i-1}, \ldots, y_{i-n_y}; x_{i-1}, \ldots, x_{i-n_x}) \tag{20}$$

It has been proved [7] [8] under very mild assumptions that any input-output process has a representation by a model of the form (20). If the system nonlinearities are polynomial in nature, this model will represent the system well for all levels of excitation. If the system nonlinearities are not polynomial, they can be approximated arbitrarily accurately by polynomials over a given range of their arguments (Weierstrass approximation theorem). This means that the system can be accurately modelled by taking the order n_p high enough. However, the model would be input-sensitive as the polynomial approximation required would depend on the data. This problem can be removed by including non-polynomial terms in the NARX model if required.

The preceding analysis unrealistically assumes that the measured data is free of noise. In reality noise arises from the truncation error associated with finite-accuracy instrumentation and arithmetic etc. In the following discussion it is allowed that noise is present. However, it is assumed that the noise signal $\zeta(t)$ is additive on the output signal $y(t)$. This constitutes no restriction if the system is linear but is generally invalid for a nonlinear system. As shown below, if the system is nonlinear the noise process can be very complex; multiplicative noise terms with the input and output are not uncommon, but can be easily accommodated by the algorithms of Billings *et al.* [7] [8] [9] [4].

Under the assumption above, the measured output has the form

$$y(t) = y_c(t) + \zeta(t) \tag{21}$$

where $y_c(t)$ is the 'clean' output from the system. If the underlying system is the Duffing oscillator of equation (16), the equation satisfied by the measured data is now

$$m\ddot{y} + c\dot{y} + ky + k_3y^3 - m\ddot{\zeta} - c\dot{\zeta} - k\zeta - k_3\zeta^3 - 3y^2\zeta + 3y\zeta^2 = x(t) \qquad (22)$$

and the corresponding discrete-time equation will contain terms of the form ζ_{i-1}, ζ_{i-2}, $\zeta_{i-1}y_{i-1}^2$ etc. Note that even simple additive noise on the output introduces cross-product terms if the system is nonlinear. Although these terms all correspond to unmeasurable states they must be included in the model. If they are ignored the parameter estimates will generally contain systematic errors, these errors are called *bias*. The system model (19) is therefore extended again by the addition of a *noise model* and takes the form

$$y_i = F^{(3)}(y_{i-1}, y_{i-2}; x_{i-2}; \zeta_{i-1}, \zeta_{i-2}) + \zeta_i \qquad (23)$$

This type of model is referred to as NARMAX (Nonlinear Auto-Regressive Moving-Average with eXogenous inputs). The NARMAX model was introduced in [7] [8] and has been developed in a sequence of papers by Billings and co-workers at Sheffield University.

Finally, the term 'moving-average' requires some explanation. Generally, for a linear system a moving-average model for the noise process takes the form

$$\zeta_i = e_i + c_1e_{i-1} + c_2e_{i-2} + \cdots \qquad (24)$$

i.e. the system noise is assumed to be the result of passing a zero-mean white noise sequence through a digital filter with coefficients $c_1, c_2, \ldots$. The terminology comes from the literature of time-series analysis. Equation (23) requires a generalisation of this concept to the nonlinear case. This is incorporated in the NARMAX model which takes the final general form

$$y_i = F^{(n_p)}(y_{i-1}, \ldots, y_{i-n_y}; x_{i-1}, \ldots, x_{i-n_x}; e_{i-1}, \ldots, e_{i-n_e}) + e_i \qquad (25)$$

In this form the noise sequence or *residual sequence* e_i is now zero-mean white noise. This allows the model to accomodate a wide class of possibly nonlinear noise terms.

3 Stucture Detection and Parameter Estimation.

Having described the basic structure of the NARMAX model, the object of the present section is give a brief description of the least-squares methods which are used to estimate the model parameters. Suppose a model of the form (17) is required for a set of measured input and output data $\{x_i, y_i; i = 1, \ldots, N\}$. Taking noise into account one has

$$y_i = a_1y_{i-1} + a_2y_{i-2} + b_1x_{i-1} + cy_{i-1}^3 + \zeta_i \qquad (26)$$

where the residual signal ζ_i will contain the output noise and an error component due to the fact that the parameter estimates may be incorrect. The least-squares estimator finds the set of parameter estimates which minimise the error function

$$J = \sum_{i=1}^{N} \zeta_i^2 \qquad (27)$$

The parameter estimates obtained will reduce the residual sequence to output noise only. If the output noise is not uncorrelated and white, a noise model is included in the NARMAX structure which reduces ζ_i to e_i, an uncorrelated white noise sequence.

The problem is best expressed in terms of matrices. Assembling each equation of the form (26) for $i = 3, \ldots, N$ into a matrix equation gives

$$\begin{vmatrix} y_3 \\ y_4 \\ \vdots \\ y_N \end{vmatrix} = \begin{vmatrix} y_2 & y_1 & x_2 & y_2^3 \\ y_3 & y_2 & x_3 & y_3^3 \\ \vdots & \vdots & \vdots & \vdots \\ y_{N-1} & y_{N-2} & x_{N-1} & y_{N-1}^3 \end{vmatrix} \begin{vmatrix} a_1 \\ a_2 \\ b_1 \\ c \end{vmatrix} + \begin{vmatrix} \zeta_3 \\ \zeta_4 \\ \vdots \\ \zeta_N \end{vmatrix} \tag{28}$$

or

$$\{y\} = [A]\{\beta\} + \{\zeta\} \tag{29}$$

in matrix notation. Throughout, matrices shall be denoted by square brackets, column vectors by curly brackets. $[A]$ is called the design matrix, $\{\beta\}$ is the vector of parameters and $\{\zeta\}$ is the residual vector. In this notation the sum of squared errors is

$$\{\zeta\}^T\{\zeta\} = (\{y\}^T - \{\beta\}^T[A]^T)(\{y\} - [A]\{\beta\}) \tag{30}$$

Minimising this expression with respect to variation of the parameters gives the well-known *normal equations* for the parameter estimates.

$$[A]^T[A]\{\beta\} = [A]^T\{y\} \tag{31}$$

which are trivially solved by

$$\{\beta\} = ([A]^T[A])^{-1}[A]^T\{y\} \tag{32}$$

provided that $[A]^T[A]$ is invertible. Because of random errors in the measurements, different samples of data will contain different noise components, consequently they will lead to slightly different parameter estimates. The parameter estimates therefore constitute a random sample from a population of possible estimates; this population being characterised by a probability distribution. Clearly, it is desirable that the expected value of this distribution should coincide with the true parameters. If such a condition holds, the parameter estimator is said to be *unbiased*. A necessary condition for the absence of bias is that the residual sequence be a zero-mean white noise signal uncorrelated with the data. The addition of a noise model reduces the residuals to such a sequence and thus allows bias-free parameter estimates. Now, given that the unbiased estimates are distributed about the true parameters, knowledge of the variance of the parameter distribution would provide valuable information about the possible scatter in the estimates. In fact, this information is readily available; the covariance matrix for the parameters is defined as

$$[C](\hat{\beta}) = E[(\{\hat{\beta}\} - E\{\hat{\beta}\}).(\{\hat{\beta}\} - E\{\hat{\beta}\})^T] \tag{33}$$

where the carets are used to emphasize the fact that quantities are estimates and the expectation E is taken over all possible estimates. The diagonal elements C_{ii} are the variances of the parameter estimates $\hat{\beta}_i$. Under a number of mild assumptions it is possible to show that, given an estimate $\{\hat{\beta}\}$,

$$[C] = \sigma_\zeta^2.([A]^T[A])^{-1} \tag{34}$$

where σ_ζ^2 is the variance of the residual sequence ζ_i obtained by using $\{\hat{\beta}\}$ to predict the output. The standard deviation for each parameter is therefore:

$$\sigma_i = \sigma_\zeta \sqrt{([A]^T[A])_{ii}^{-1}} \tag{35}$$

If the parameter distributions are Gaussian, standard theory yields a 95% confidence interval of $\{\hat{\beta}\} \pm 1.96\{\sigma\}$, i.e. there is a 95% probability that the true parameters fall within this interval.

In practice, direct solution of the normal equations via (32) is not recommended as problems can arise if the matrix $[A]^T[A]$ is close to singularity. Suppose that the RHS of equation (31) has a small error $\{\delta y\}$ due to roundoff say, the resulting error in the estimated parameters is given by

$$\{\delta\beta\} = ([A]^T[A])^{-1}[A]^T\{\delta y\} \tag{36}$$

As the elements in the inverted matrix are inversely proportional to the determinant of $[A]^T[A]$, they can be arbitrarily large if $[A]^T[A]$ is close to singularity. As a consequence, parameters with arbitrarily large errors can be obtained. This problem can be avoided by use of more sophisticated techniques. The near-singularity of the matrix $[A]^T[A]$ will generally be due to correlations between its columns (recall that a matrix is singular if two columns are equal) i.e. correlations between model terms. It is possible to transform the set of equations (32) into a new form in which the columns of the design matrix are uncorrelated, thus avoiding the problem. This 'orthogonal' version of the least-squares procedure is used throughout this work. A comprehensive description of the theory is given in [9] or [4].

In practice, it is unusual to know which terms should be in the model. This is not too much of a problem if the system under study is known to be linear; the number of possible terms is a linear function of the numbers of lags n_y, n_x and n_e. However, if the system is nonlinear, the number of possible terms increases *combinatorially* with increasing numbers of lags. In order to reduce the computational load on the parameter estimation procedure it is clearly desirable to determine which terms should be included. Also, experience indicates that a final model containing ten to fifteen terms is usually adequate. With this in mind, the problem of *structure detection* is now considered. As the initial specification of a NARMAX model (25) includes all product terms up to order n_p, the model-fitting procedure needs to include some means of determining which of the possible terms are significant so that the remainder can safely be discarded. The measure of significance used in the orthogonal estimation procedure referred to above is called the error-reduction ratio or ERR [4]; an equivalent procedure based on the normal equations is presented here. In order to determine whether a term is an important part of the model, a significance factor can be defined as follows. Each model term $\theta(t)$, e.g. $\theta(t) = y_{i-2}$ or $\theta(t) = y_{i_1}^2 x_{i-2}$, can be used on its own to generate a time-series which will have variance σ_θ^2. The significance factor s_θ is then defined by

$$s_\theta = 100\frac{\sigma_\theta^2}{\sigma_y^2} \tag{37}$$

where σ_y^2 is the variance of the estimated output, i.e. the sum of all the model terms. Roughly speaking, s_θ is the percentage contributed to the model variance by the

term θ. Having estimated the parameters the significance factors can be determined for each term; all terms which contribute less than some threshold value s_{min} to the variance can then be discarded. Although the description above captures the essence of the ERR, the procedure is only correct when used with the orthogonal estimator. This is because all terms in the orthogonal basis are uncorrelated with each other. If one were to use the procedure on terms with intercorrelations one might observe two or more terms which appear to have a significant variance which actually cancelled to a great extent when added together.

Finally, some remarks are required on the subject of parameter estimation if a noise model is necessary. The situation is complicated by the fact that the noise signal is unmeasurable. In this case, an initial fit is made to the data without a noise model, the model predicted output is then subtracted from the measured output to give an estimate of the noise signal. This allows the re-estimation of parameters, including now the noise model parameters. The procedure, fit model - predict output - estimate noise signal, is repeated until the parameters converge.

This concludes the discussion on forming the NARMAX model. Having obtained a model, it is important to have some means of testing its validity; this will form the subject of the next section.

4 Model Validity.

Having obtained a NARMAX model for a system, the next stage in the identification procedure is to determine if the structure is correct and the parameter estimates are unbiased. It is important to know if the model has successfully captured the system dynamics so that it will provide good predictions of the system output for different input excitations, or if it has simply fitted the model to the data; in which case it will be of little use since it will only be applicable to one data set. Three basic tests of the validity of a model are applied in the present work; they are described below in increasing order of stringency. In the following, y_i denotes a measured output while $\hat{y}_i$ denotes an output value predicted by the model.

4.1 One-Step-Ahead Predictions

Given the NARMAX representation of a system

$$y_i = F^{(n_p)}(y_{i-1}, \ldots, y_{i-n_y}; x_{i-1}, \ldots, x_{i-n_x}; e_{i-1}, \ldots, e_{i-n_e}) + e_i \qquad (38)$$

the one-step-ahead prediction or *curve-fit* of y_i is made using measured values for all past inputs *and* outputs. Estimates of the residuals are obtained from the expression $\hat{e}_i = y_i - \hat{y}_i$ i.e.

$$\hat{y}_i = F^{(n_p)}(y_{i-1}, \ldots, y_{i-n_y}; x_{i-1}, \ldots, x_{i-n_x}; \hat{e}_{i-1}, \ldots, \hat{e}_{i-n_e}) \qquad (39)$$

The one-step-ahead series can then be compared to the measured outputs. Good agreement is clearly a necessary condition for model validity.

4.2 Model Predicted Output.

In this case, the inputs are the only measured quantities used to generate the model output, i.e.

$$\hat{y}_i = F^{(n_p)}(\hat{y}_{i-1}, \ldots, \hat{y}_{i-n_y}; x_{i-1}, \ldots, x_{i-n_x}; 0, \ldots, 0) \tag{40}$$

The zeroes are present because the prediction errors will not generally be available when one is using the model to predict output. In order to avoid a misleading transient at the start of the record for $\hat{y}$, the first n_y values of the measured output are used to start the recursion. As above, the estimated outputs must be compared with the measured outputs, with good agreement a necessary condition for accepting the model. It is clear that this test is stronger than the previous one; in fact the one-step-ahead predictions can be excellent in some cases when the model predicted output shows complete disagreement with the measured data.

4.3 Correlation Tests.

These represent the most stringent of the validity checks. The appropriate reference is [10]. The correlation function $\phi_{uv}(k)$ for two sequences of data u_i and v_i is defined by

$$\phi_{uv} = E(u_i v_{i+k}) \approx \frac{1}{N-k} \sum_{i=1}^{N-k} u_i v_{i+k} \tag{41}$$

For a linear system it can be shown [10] that necessary conditions for model validity are

$$\phi_{ee}(k) = \delta_{0k} \tag{42}$$

$$\phi_{xe}(k) = 0 \quad \forall k \tag{43}$$

The first of these conditions is true only if the residual sequence e_i is a white noise sequence. It is essentially a test of the adequacy of the noise model whose job it is to reduce the residuals to white noise. If the noise model is correct, the system parameters should be free from bias. The second of the conditions above states that the residual signal is uncorrelated with the input sequence x_i i.e. the model has completely captured the component of the measured output which is correlated with the input. Another way of stating this requirement is that the residuals should be unpredictable from the input.

In the case of a nonlinear system it is sometimes possible to satisfy the requirements above even if the model is invalid. It can be shown [10] that an exhaustive test of the fitness of a nonlinear model requires the evaluation of three additional correlation functions. The extra conditions are

$$\phi_{e(ex)}(k) = 0 \quad \forall k \geq 0 \tag{44}$$

$$\phi_{x^2 'e}(k) = 0 \quad \forall k \tag{45}$$

$$\phi_{x^2 'e^2}(k) = 0 \quad \forall k \tag{46}$$

The dash which accompanies x^2 above indicates that the mean has been removed. Normalised estimates of all the correlation functions above are obtained using

$$\hat{\phi}_{uv}(k) = \frac{\frac{1}{N-k}\sum_{i=1}^{N-k} u_i v_{i+k}}{\{E(u_i^2)E(v_i^2)\}^{\frac{1}{2}}} \qquad k \geq 0 \tag{47}$$

with a similar expression for $k < 0$. The normalised expression is used because it allows a simple expression for the 95% confidence interval for a zero result, namely $\pm 1.96/\sqrt{(N)}$. The confidence limits are required because the estimate of ϕ_{uv} is made only on a finite set of data; as a consequence it will never be truly zero. The model is therefore considered adequate if the correlation functions described above fall within the 95% confidence limits. These limits are indicated by a dashed line when the correlation functions are shown in the following sections.

4.4 Chi-Squared Test.

One final utility can be mentioned. If the model fails the validity tests one can compute a statistic η [4] for a given term *not* included in the model to see if it should be present. The test is specifically developed for nonlinear systems and is based on chi-squared statistics. A number of values of the statistic for a specified term are plotted together with the 95% confidence limits. If values of the statistic fall *outside* the limits, the term should be included in the model and it is necessary to re-estimate parameters accordingly. Examples of all the test procedures described above will be given in the following section.

5 Analysis of a Simulated Fluid Loading System.

In order to demonstrate the concepts described in previous sections, the techniques are now applied to simulated data from the Morison equation (1). The first problem is to determine an appropriate discrete-time form. The conditions $\rho = 1, D = 2$ are imposed giving the equation

$$F(t) = \pi C_m \dot{u} + C_d u(t)|u(t)| \tag{48}$$

where $F(t)$ is the system output and $u(t)$ will be the input. Using the difference formula (9) one obtains the discrete form

$$F_i = \frac{\pi C_m}{\Delta t}(u_i - u_{i-1}) + C_d u_i|u_i| \tag{49}$$

The basic form of the NARMAX procedures used here utilises polynomial model terms. For the sake of simplicity, the $u|u|$ term in the simulation model is replaced by a cubic approximation,

$$u_i|u_i| = \alpha u_i + \beta u_i^3 + O(u_i^5) \tag{50}$$

The coefficients α and β are obtained by a simple least-squares argument which is given in Appendix A. Substituting (50) into (49) yields the final NARMAX form of Morison's equation

$$F_i = (\alpha C_d + \frac{\pi C_m}{\Delta t})u_i - \frac{\pi C_m}{\Delta t}u_{i-1} + \beta C_d u_i^3 \tag{51}$$

or

$$F_i = a_1 u_i + a_2 u_{i-1} + a_3 u_i^3 \tag{52}$$

This is the model which was used for the simulation of force data. A velocity signal was used which had a uniform spectrum in the range 0 Hz to 20 Hz. This was obtained by generating 50 sinusoids each with an amplitude of 5.0 units spaced uniformly in frequency over the specified range; the phases of the sinusoids were taken to be random numbers uniformly distributed on the interval $[0, 2\pi]$. The sampling frequency was chosen to be 100 Hz, giving five points per cycle of the highest frequency present. It should be noted that the absolute frequencies have no meaning here, the important quantity is normalised frequency i.e. the ratio of frequency to sampling frequency. The amplitude for the sinusoids was chosen so that the nonlinear term in (52) would contribute approximately 5% to the total variance of F. The uniform spectrum is chosen here for convenience, a more realistic simulation would require the imposition of a Pierson-Moskowitz or JONSWAP spectrum [12]. However, the uniform spectrum is adequate for illustrative purposes. The simulated velocity and force data is displayed in Figure 1. In order to show the accuracy of the cubic approximation (50) over the range of velocities generated, the function $u|u|$ is plotted in Figure 2 together with the cubic curve fit; the agreement is very good. The values of the exact NARMAX coefficients for the data were $a_1 = 661.49$, $a_2 = -628.32$ and $a_3 = 0.015479$.

In order to demonstrate fully the capabilities of the procedures, a *coloured* noise signal ζ was added to the force data. The noise model chosen was

$$\zeta_i = 0.222111e_{i-1} - e_{i-2} + e_{i-3} \tag{53}$$

where e_i was a Gaussian white noise sequence. The variance of $e(t)$ was chosen in such a way that the overall signal to noise ratio σ_F/σ_ζ would be equal to 5.0. This corresponds to the total signal containing approximately 17% noise. This is comparatively low, a benchtest study [13] showed that the NARMAX procedures could adequately identify Morison type systems with the signal to noise ratio as high as unity.

The first attempt to model the data assumed the linear structure

$$F_i = a_1u_i + a_2u_{i-1} \tag{54}$$

The resulting parameter estimates were $a_1 = 687.7$ and $a_2 = -628.29$ with standard deviations $\sigma_{a_1} = 4.6$ and $\sigma_{a_2} = 4.6$. The estimated value of a_1 is 5.7 standard deviations away from the true parameter, this indicates bias. The reason for the overestimate is that the u_i^3 term which should have been included in the model is strongly correlated with the u_i term; as a consequence the NARMAX model can represent some of the nonlinear behaviour by adding an additional u_i component. It is because of effects like this that data from nonlinear systems can sometimes be adequately represented by linear models. However, such models will be input-dependent as changing the level of input would change the amount contributed by the nonlinear term and hence the estimate of a_1.

The one-step-ahead predictions for the model were observed to be excellent. The model predicted output, shown in Figure 3, also agreed well with the simulation data. However, if the correlation tests are consulted (Figure 4), both ϕ_{ee} and $\phi_{u^2'e}$ show excursions outside the 95 % confidence interval. The first of these correlations indicates that the system noise is inadequately modelled, the second shows that the model does not take nonlinear effects correctly into account. This example shows clearly the utility of the correlation tests. Figure 5 shows the results of chi-squared tests on the terms u_i^3 and e_{i-1}; in both cases the graphs are completely outside the

95 % confidence interval; this shows that these terms should have been included in the model. A further test showed that the e_{i-2} term should also have been included.

In the second attempt to identify the system, the correct process model was assumed,

$$F_i = a_1 u_i + a_2 u_{i-1} + a_3 u_i^3 \tag{55}$$

but no noise model was included. The resulting parameter estimates were $a_1 = 659.86$, $a_2 = -627.53$ and $a_3 = 0.015743$ with standard deviations $\sigma_{a_1} = 5.9$, $\sigma_{a_2} = 4.5$ and $\sigma_{a_3} = 0.002$. The inclusion of the nonlinear term in the model has removed the principal source of the bias on the estimate of a_1 and all estimates are now within one standard deviation of the true results. The one-step-ahead predictions and model predicted outputs for this model showed no visible improvements over the linear model. However, the correlation test showed $\phi_{u^2 e}$ to be within the confidence interval, indicating that the nonlinear behaviour is now correctly captured by the model. As expected $\phi_{ee}(k)$ is still non-zero for $k > 0$ indicating that a noise model is required. This conclusion was reinforced by the chi-squared tests for e_{i-1} and e_{i-2} which showed that these terms should be included.

The final attempt to model the system used the correct nonlinear structure and included a noise model with linear terms $e_{i-1}, \ldots, e_{i-5}$. The parameter estimates were accurate once more. The most significant noise term was found to be e_{i-2}; if just this term was included in the model the correlation tests (Figure 6) improved but still showed an excursion outside the confidence limits for $\phi_{ee}(k)$ at $k = 1$. Generally, if $\phi_{ee}(k)$ leaves the confidence interval at lag k, a term e_{i-k} should be included in the model. In this case the tests show that e_{i-1} should be included, and this confirms the result of the chi-squared test in Figure 5.

This simulation illustrates nicely the suitability of NARMAX procedures for the study of fluid loading forces. More importantly it shows clearly the need for the correlation tests, it is not sufficient to look at agreement between model predicted data and measured data. The estimation procedures can still allow a good representation of a given data set even if the model structure is wrong, simply by biasing the parameter estimates for the terms present. However, in this case the model is simply a curve fit to a specific data set and will be totally inadequate for prediction on different inputs.

6 Analysis of U-tube Data.

The U-tube data (previously discussed in [2]) were obtained by digitising the force time-history figures from published papers and reports. The data sets examined are from the experimental study by Obasaju *et al.* [14]. In the experiment, at various values of KC, the time-history of the force on a cylinder in a regular planar oscillatory flow was measured. For each KC value considered, two types of force histories were distinguised in the experiment. Elements of the first class of force histories were produced by carefully averaging over cycles which exhibited the same form or mode of vortex shedding. Elements of the second class were obtained by averaging over *all* cycles, irrespective of the mode of vortex shedding. It is the second class which is considered here. For a fixed β value of 417, the KC values for which averaged force cycles were available were 3.31, 6.48, 11.88, 17.5 and 34.68.

In order to form a basis for comparison the data was first examined by forcing the model structure to be that of the discrete-time Morison equation (52)

The parameter estimates for the model have no physical meaning. However, as the coefficients a_1, a_2 and a_3 are simple functions of C_d, C_m and Δt the sampling interval, it is possible to pass from the discrete-time parameters to the more physical continuous-time parameters. However, as it is the model structures which are of interest here the parameter estimates are not converted.

It is useful to have some numerical measure of the closeness of fit of the model. The one adopted here is the normalised mean-square error or MSE. This is defined by

$$MSE = 100\frac{\sigma_e^2}{\sigma_F^2} \tag{56}$$

where $e(t)$ is the residual signal decribed in Section 2, which represents that component of the measured $F(t)$ which is not accounted for by system model or noise model.

The Morison model was fitted to each of the five samples of data and the model MSEs are given in Table 1. As one might expect, the Morison equation coped well with the data for the two lowest KC values so only the comparisons between measured data and model predicted output for the remaining data sets are shown (Figures 7-9). In all cases the model validity tests show values outside the dashed confidence limits, this indicates clearly that the model is inadequate.

For the next stage of the analysis, the structure detection routines were used to determine which terms should be in the model. The parameter tables for the resulting models are given in Tables 3 to 6. The tables also show the ERR value for the term and the estimated standard deviation of the parameter. In all cases the MSE is reduced, the results are summarised in Table 7.

The comparisons between measured data and model predicted output for the higher KC data sets are given in Figures 10 to 12 with the corresponding correlation test results. The improvement in the predictions is evident. The model validity tests also show a great deal of improvement, in almost all cases the results are within the confidence limits for a valid model.

The interpretation of the models is not clear, in each case there are many more terms than in the discrete Morison equation. Also, the terms linear in u required by Morison's equation are not always present, they are usually replaced by terms linear in y (i.e. F). This may be due to the oversampling effect described in [13] where it was shown that sampling rates higher than 5 to 10 points per cycle tended to cause the parameter estimation routines to select output terms rather than input terms, the result being an excessively complicated model. Unfortunately, oversampling is inevitable for the U-tube data. In order to use the estimation routines one must have approximately 50 input/output pairs. As the U-tube data is digitised from figures containing one cycle, one is forced to adopt an effective sampling rate of more than 50 points per cycle. Although an oversampled model can be perfectly adequate for prediction purposes, it may be very difficult to associate the model terms with terms in the underlying continuous-time equations of motion of the system. It is interesting to note that the predominant nonlinear term is always u^3 or in one case y^3. However, beyond this, the number and type of the nonlinear terms changes for each data set. This is not particularly surprising if one assumes that no simple extension of the Morison equation exists; the cubic terms are always present because they are a part of the drag component, the source of the remaining nonlinearity is largely the vortex shedding [2] and it is well known that the pattern or mode of shedding can change dramatically as KC changes.

It is interesting that for the $KC = 17.5$ data (Table 5), the routines actually select the terms for a discrete form of the Duffing-Morison equation [2],

$$\alpha_1 \ddot{F} + \alpha_2 \dot{F} + F + \alpha_3 F|F| = \frac{1}{2}\rho D C_d u(t)|u(t)| + \frac{1}{4}\pi\rho D^2 C_m \dot{u}(t) \qquad (57)$$

although if $u(t-1)$ and $u(t-3)$ truly represented the discrete version of the derivative $\dot{u}$, their coefficients would be equal and opposite, which is not the case here. As a result, one might tentatively conclude that the Duffing-Morison equation cannot be the correct extended model for if it were, the algorithms would determine the correct parameters given the correct terms.

In conclusion, the above results show that it is possible to improve greatly on the predictive capability of Morison's equation at the expense of introducing models with terms which have no clear physical meaning e.g. $F_{i-3}u_{i-3}$. Also, the model *structure* and parameters change with KC as opposed to the Morison case where the structure has been incorrectly forced onto the data. The danger of this latter approach is that the values of the parameters obtained will be biased and therefore of questionable value. A further, more important caveat is that the inputs (i.e. flow velocities) to the systems considered here are all sinusoids or narrow-band signals, as a consequence they do not excite the system except over small frequency intervals. In the terminology of system identification the inputs are not *persistently exciting*, they are unlikely to generate all the possibilities for system response. As a consequence the results above should be interpreted with great care.

7 Analysis of Wave Flume Data.

The data was obtained from the Delta flume of the De Voorst facility of Delft Hydraulics. The particular data considered here comes from the run OA1F1 which used a fixed smooth cylinder. The unidirectional wave profiles were generated so that the the surface elevation spectrum approximated to a JONSWAP spectrum. More details of the experiment can be found in [16] which contains an exhaustive wave-by-wave Morison analysis of the full De Voorst data set. In the experiment, the velocity signal was obtained from electromagnetic flowmeters placed adjacent to the cylinder at the same distance from the wave maker. The forces were recorded from force sleeves placed at three levels (Stations 2,3 and 4) on the cylinder. The data from Station 2 had to be discarded as the sleeve fell within the crest to trough region of the wave. Of those remaining, Station 3 was nearest to the surface while fully immersed and was consequently subjected to the highest nonlinear forces. For this reason data from Station 3 was used in the following analysis.

Because of a delay in the instrumentation, the velocity data led the force data by 5.6 sampling instants in each record. This delay was reduced to 0.4 instants by shifting the velocity arrays by six units. After the analysis described below was carried out, the effect of the residual lag was investigated by using an interpolation procedure to remove it. Some of the analysis was then repeated. The results were almost identical; slightly different parameters were observed and the MSE values for the models increased slightly, possibly due to the approximate nature of the interpolation. Because of this the results shown below are for the data with the residual delay of 0.4 instants.

A systematic and exhaustive analysis, including structure detection, of the full OA1F1 data set (over one hundred thousand input/output pairs), would be too time-consuming. Also, a preliminary Morison analysis showed that the fluid loading

forces are predominantly linear. For these reasons only the 'most nonlinear' data were analysed. In order to identify a correct nonlinear model for any system it is necessary that the nonlinearity be sufficiently excited. In this case this corresponds to when the velocity is high. A further useful sign of nonlinearity is the size of the out-of-line component of the force. For this reason, the data for analysis was chosen to be centred about the instant of the maximum transverse force excursion.

As with the U-tube data, the De Voorst data is oversampled from the point of view of parameter estimation. Fourier analysis of the input and output data showed spectra with a narrow-banded aspect centred about the frequency 0.2 Hz (Figure 13), while the sampling frequency for the data was 20 Hz. Because there is such a large amount of the data one can effectively reduce the sampling frequency by decimating the data. A simple calculation shows that if one assumes a highest frequency of interest of 0.4 Hz, one can decimate the data by factors of up to 24 without undersampling. The price one pays for this freedom is that decimation reduces the proportion of significantly nonlinear data in a given sample. Results will be presented for decimation factors of 1, 2 and 4, corresponding to sampling freqencies f_s of 20Hz, 10Hz and 5Hz respectively.

As before, a discrete Morison model was fitted to the data to serve as a basis for comparison. The resulting model prediction errors are given in Table 8 and the corresponding parameters are given in Table 9. The model predicted output and the correlation test results for the 20Hz data are given in Figure 14.

The data were then analysed using the structure detection algorithms to determine which terms should be present. The resulting model prediction errors are shown in Table 10. The parameter tables for the three models are given in Table 11. The presence of the terms linear in y as the dominant terms in each model can possibly be attributed to oversampling, this is supported by the fact that the ERR contribution of the term $y(t-1)$ which measures the contribution of the term to the model, falls steadily as the effective sampling frequency decreases. However, it must be argued that these terms are necessary given that the model validity tests show a distinct improvement on the Morison results. The main feature of interest is that the next most important terms always constitute a discrete Morison submodel, i.e the linear terms $u(t-1)$ and $u(t-2)$ always appear as a derivative pair (equal and opposite coefficients) and the most significant nonlinear term is always u^3 for some lag value. This was also observed at data with the higher decimation factors 8 and 16.This would seem to indicate that one cannot do much better than Morison's equation for the De Voorst OA1F1 data. This is not surprising in view of the fact that the linear inertia component of the force dominates throughout. The model predicted output and the correlation test results for the 20Hz data is given in Figure 15. There is no visible improvement in the fit to the prediction (c.f. Figure 14). However, the model validity test show a distinct improvement.

As with U-tube data, the De Voorst data is not ideal for system identification purposes. However, one can draw a more definite conclusion in this case which is that Morison's equation is perfectly adequate to describe the fluid loading forces in this particular test.

8 Analysis of a Directional Sea State.

The U-tube and De Voorst data is valuable in that it is of high quality and enables new model structures of the force equation with vortex shedding to be investigated. The flow situations are however idealised with Reynolds numbers well below full scale

values.

In this section the new model structures are fitted to forces and velocities measured on the Christchurch Bay Tower described in [17]. The same cylinder was used in the De Voorst tests but the sea states have greater wave heights (up to 7m against 2m at De Voorst) and are directional with a prominent current. The velocities were measured with calibrated perforated ball meters attached at a distance of 1.228m from the cylinder axis. This will not give the exact velocity at the centre of the force sleeve unless waves are unidirectional with crests parallel to the line joining the velocity meter to the cylinder. This is called the Y direction and the normal to this, the X direction. The waves are however always varying in direction so in order to facilitate the fitting of a single-input-single-output (SISO) model, the data was chosen from an interval when the oscillatory velocity in the X direction was large and that in the Y direction small. A sample of 1000 points fitting these criteria is shown in Figure 16. The sampling frequency for this data set was 10 Hz. It can be seen that the current is mainly in the Y direction. In this case the velocity ball is upstream of the cylinder and interference by the wake on the ball will be as small as possible with this arrangement. Using RMS velocities, the KC values in the X and Y directions are 19.7 and 4.85 respectively. The magnitude of the velocity is shown in Figure 17 together with the angle of the velocity vector relative to the X direction. This angle shows considerable variation; however, the larger angles are simply due to the fact that the predominant current direction is the Y direction so the velocity vector will be directed along Y whenever there is a zero-crossing in the X-component of the velocity. Parameter estimation methods in general are very sensitive to phase differences or delays between input and output; the directionality here induces a time-varying delay so some difficulty was anticipated. It is clear that this data is not of the same quality as that section 7, however, it was sufficiently reliable for a number of positive results to be obtained.

As in previous sections, the discrete form of Morison's equation was fitted to the data to serve as a basis for comparison. The coefficients are presented in Table 12, note that the coefficients of u_i and u_{i-1} (respectively u(t-1) and u(t-2) in the table) are almost equal and opposite indicating that they constitute the discretisation of an inertia term $\dot{u}$. The MSE for the model is 21.43 which indicates significant disagreement with reality. The model predicted output is shown in Figure 18 together with the correlation tests. One concludes that the model is inadequate.

The data was then analysed using the structure detection algorithm to determine which terms should be included in the model. A nonlinear noise model was included. The resulting model is given in Table 13. As in the case of the U-tube data of Section 6, a complex model was obtained which includes terms with no clear physical interpretation. The fact that such a model is required can be offered in support of the conclusion that the inadequacy of Morison's equation is due to the gross vortex shedding effects which were observed in the U-tube experiments but not in the De Voorst wave flume [2]. The model predicted output and correlation tests are shown in Figure 19. Although the validity tests show a great deal of improvement, the model predicted output appears to be worse. This is perfectly understandable; one of the effects of correlated noise (indicated by the the function $\phi_{\varepsilon\varepsilon}$ in Figure 18) is to bias the model coefficients so that the model fits the data rather than the underlying system. In this case the model predicted output is actually accounting for some of the system noise; this is clearly incorrect. When the noise model is added to reduce the noise to a white sequence, the unbiased model no longer predicts the noise component and the model predicted output appears to represent the data less well.

This is one reason why the MSE adopted here makes use of the residual sequence e_i rather than the prediction errors ζ_i. Figure 20 shows a comparison between the white residual signal and the coloured prediction errors. In this case, the MSE is 0.70735 which shows a marked improvement over Morison. The fact that the final correlation function in Figure 19 still indicates problems with the model can probably be attributed to the time-dependent phase relationship between input and output described above. It is possible that this could be improved with further analysis.

The results here seem to indicate again that there is no simple extension to Morison's equation which allows a direct physical interpretation of the additional terms. The Christchurch Bay data shows a strong resemblance to the U-tube data in this respect.

9 Conclusion.

The results presented above for the oscillatory flow data and the directional sea data offer evidence that there is no simple extension to Morison's equation for prediction purposes which allows a physical interpretation of the additional terms - at least in the disrete-time case. In the case of the De Voorst data, Morison's equation gives acceptably accurate predictions over almost the whole data set simply because the data is linear, inertia-dominated. In the case of the U-tube data, Morison is visibly inadequate for detailed prediction; however, the models identified here which *can* predict accurately change their structure as KC and consequently the vortex shedding patterns change. This allows the conclusion that Morison's equation fails when there is gross vortex shedding. In this case Morison's equation can still be regarded as useful as it provides at least a reasonable estimate of force whilst keeping the same model structure. One might argue that the conditions in a U-tube are artificial and the sort of nonlinear behaviour displayed there would not occur in real situations. For this reason it was important to analyse data collected from real seas with comparable KC values. The models obtained from analysis of the Christchurch Bay data show the same type of structure as those from the U-tube. This allows the conclusion that vortex shedding effects are significant, which is consistent with the more heuristic reasoning in [2].

These conclusions must be regarded as tentative for two reasons. Firstly, the data is not ideally designed for use with system identification methods. Oversampling is a problem in most of the data presented here, the effect of this is simply to produce an overly complex model, the validity of the model is not affected. Also, the narrow-band excitations are suboptimal for parameter identification purposes. Secondly, the discrete NARMAX form for a continuous-time system is not unique; the models presented here, while differing considerably in their structure, may all reflect a common underlying differential equation model. In fact, the question of uniqueness will be taken up in the second part of this study where it will be shown that the problem can be largely circumvented by passing to the frequency-domain.

Acknowledgements.

Thanks are due to Delft Hydraulics for access to the wave force data obtained in the Delta flume in their De Voorst facility. This data was provided with the assistance of Malcolm Birkinshaw of the Health and Safety Executive and Professor Peter Bearman and Martin Davies of Imperial college. In particular, the help provided by Martin

Davies in translating data into a useful format is much appreciated. Thanks are also due to Dr. Emmanuel Obasaju for making available unpublished data from his experimental work undertaken as a research associate at Imperial College. This project is supported by the Offshore Safety Division of the Health and Safety Executive through the Marine Technology Directorate's managed programme on the Behaviour of Fixed and Compliant Offshore Structures. This paper will comprise part of the final report to the Health and Safety Executive (to be published by HMSO).

References

[1] Morison (J.R.), O'Brien (M.P.), Johnson (J.W.) & Schaf (S.A.) 1950 *Petroleum Transactions* **189** pp.149-157. The force exerted by surface waves on piles.

[2] Stansby (P.K.), Worden (K.), Billings (S.A.) & Tomlinson (G.R.) 1991 *To appear in Applied Ocean Research.* Improved wave force classification using system identification.

[3] Sarpkaya (T.) 1981 *US Naval Civil Engineering Laboratory Report no. CR 82.008.* Morison's equation and the wave forces on offshore structures.

[4] Chen (S.), Billings (S.A.) & Liu (Y.P.) 1987 *International Journal of Control* **50** pp.1873-1896. Orthogonal least-squares methods and their application to nonlinear system identification.

[5] Billings (S.A.) & Tsang (K.M.) 1989 *Mechanical Systems and Signal Processing* **3** pp.341-359. Spectral analysis for nonlinear systems, part II: Interpretation of nonlinear frequency response functions.

[6] Worden (K.), Billings (S.A.), Stansby (P.K.) & Tomlinson (G.R.) 1991 *Submitted to Journal of Fluids and Structures.* Identification of nonlinear wave forces. Part II. Frequency-domain analysis.

[7] Leontaritis (I.J.) & Billings (S.A.) 1985 *International Journal of Control* **41** pp.303-328. Input-output parametric models for Nonlinear systems. Part I: deterministic nonlinear systems.

[8] Leontaritis (I.J.) & Billings (S.A.) 1985 *International Journal of Control* **41** pp.329-344. Input-output parametric models for Nonlinear systems. Part II: stochastic nonlinear systems.

[9] Korenburg (M.), Billings (S.A.) & Liu (Y.P.) 1988 *International Journal of Control* **51** pp.193-210. An orthogonal parameter estimation algorithm for nonlinear stochastic systems.

[10] Billings (S.A.), Chen (S.) & Backhouse (R.J.) 1989 *Journal of Mechanical Systems and Signal Processing* **3** pp.123-142. Identification of linear and nonlinear models of a turbocharged automotive diesel engine.

[11] Leontaritis (I.J.) & Billings (S.A.) 1987 *International Journal of System Science* **18** pp.189-202. Experimental design and identifiability of nonlinear systems.

[12] Chakrabarti (S.K.) 1987 *Hydrodynamics of Offshore Structures.* Computational Mechanics Publications, Southampton and Springer-Verlag, Heidelberg.

[13] Worden (K.), Billings (S.A.), Stansby (P.K.) & Tomlinson (G.R.) 1990 *Confidential Technical Report to Department of Energy.* Parametric modelling of fluid loading forces II.

[14] Obasaju (E.D.), Bearman (P.W.) & Graham (J.M.R.) 1988 *Journal of Fluid Mechanics* **196** pp.467-494. A study of forces, circulation and vortex patterns around a circular cylinder in oscillating flow.

[15] Klopman (G.) & Kostense (J.K.) 1989 in *Water Wave Kinematics* Torum & Gudmestad (eds.) NATO ASI series E 178. The loading on a vertical cylinder in random waves at high Reynolds numbers.

[16] Davies (M.J.S.), Graham (J.M.R.), & Bearman (P.W.) 1990 in *Environmental Forces on Offshore Structures and Their Prediction* pp.113-136. Kluwer Academic Press.

[17] Bishop (J.R.) 1979 *National Maritime Institute report no. NMI R57* Aspects of large scale wave force experiments and some early results from Christchurch Bay.

Appendix A. Approximating $u|u|$ by a Cubic Polynomial.

The basic problem is to determine the best, in the least squares sense, cubic representation of the function $u|u|$ over a given interval $a \leq u \leq b$. Because $u|u$ is an odd function, one immediately has

$$u|u| \approx \alpha u + \beta u^3 + O(u^5) \tag{58}$$

The coefficient estimates are fixed by minimising the error functional

$$J(\alpha, \beta) = \int_a^b du(u|u| - \alpha u - \beta u^3)^2 \tag{59}$$

with respect to α and β. One obtains for the α variation

$$\frac{\partial J}{\partial \alpha} = 0 \Rightarrow A_{11}\alpha + A_{12}\beta - B_1 = 0 \tag{60}$$

where

$$A_{11} = \int_a^b u^2 du = \frac{1}{3}(b^3 - a^3) \tag{61}$$

$$A_{12} = \int_a^b u^4 du = \frac{1}{5}(b^5 - a^5) \tag{62}$$

$$B_1 = \int_a^b u^2|u| du = \frac{1}{4}(b^4 - a^4) \tag{63}$$

while varying β yields

$$\frac{\partial J}{\partial \beta} = 0 \Rightarrow A_{21}\alpha + A_{22}\beta - B_2 = 0 \tag{64}$$

where

$$A_{21} = \int_a^b u^4 du = \frac{1}{5}(b^5 - a^5) = A_{12} \tag{65}$$

$$A_{22} = \int_a^b u^6 du = \frac{1}{7}(b^7 - a^7) \tag{66}$$

$$B_2 = \int_a^b u^4 |u| du = \frac{1}{6}(b^6 - a^6) \tag{67}$$

The parameter estimates are now obtained by solving the linear simultaneous equations (A.3) and (A.7). The result being

$$\alpha = \frac{A_{12}B_2 - A_{22}B_1}{A_{21}A_{12} - A_{11}A_{22}} \tag{68}$$

$$\beta = \frac{A_{21}B_1 - A_{11}B_2}{A_{21}A_{12} - A_{11}A_{22}} \tag{69}$$

Given a set of time data u(t), a convenient choice for the approximating interval is $[-u_{rms}, u_{rms}]$, in this case

$$u|u| \approx \frac{5u_{rms}}{16}u + \frac{35}{48u_{rms}}u^3 \tag{70}$$

Figure Captions

Figure 1. Simulated velocity and force signals for the coloured noise study.

Figure 2. Comparison between $u|u|$ and cubic approximation.

Figure 3. Coloured noise study: model predicted output for linear process model - no noise model.

Figure 4. Coloured noise study: correlation tests for linear process model - no noise model.

Figure 5. Coloured noise study: chi-squared tests for linear process model - no noise model.

Figure 6. Coloured noise study: correlation tests for nonlinear process model with linear noise model.

Figure 7. Discrete Morison fit to $KC = 11.88$ U-tube data. (a) Model predicted output. (b) Correlation tests.

Figure 8. Discrete Morison fit to $KC = 17.5$ U-tube data. (a) Model predicted output. (b) Correlation tests.

Figure 9. Discrete Morison fit to $KC = 34.68$ U-tube data. (a) Model predicted output. (b) Correlation tests.

Figure 10. NARMAX fit to $KC = 11.88$ U-tube data. (a) Model predicted output. (b) Correlation tests.

Figure 11. NARMAX fit to $KC = 17.5$ U-tube data. (a) Model predicted output. (b) Correlation tests.

Figure 12. NARMAX fit to $KC = 34.68$ U-tube data. (a) Model predicted output. (b) Correlation tests.

Figure 13. Velocity Power Spectral Density for De Voorst data.

Figure 14. Discrete Morison fit to sample of De Voorst data. (a) Model predicted output. (b) Correlation tests.

Figure 15. NARMAX fit to sample of De Voorst data. (a) Model predicted output. (b) Correlation tests.

Figure 16. X and Y components of velocity for sample of Christchurch Bay data.

Figure 17. 'In-line' component of velocity and angle between velocity and X direction for sample of Christchurch Bay data.

Figure 18. Discrete Morison fit to sample of Christchurch Bay data. (a) Model predicted output. (b) Correlation tests.

Figure 19. NARMAX fit to sample of Christchurch Bay data. (a) Model predicted output. (b) Correlation tests.

Figure 20. Residual and deterministic prediction error for NARMAX fit to sample of Christchurch Bay data.

KC	MSE
3.31	0.048
6.48	0.283
11.88	6.038
17.50	0.536
34.68	1.495

Table 1: MSE values for discrete Morison fit to U-tube data.

Model Term	Parameter	ERR	St.Dev.
F_{i-1}	0.86255e+00	0.99075e+00	0.11296e+00
u_{i-3}	-0.97219e+01	0.90033e-02	0.21840e+01
F_{i-2}	-0.32474e+00	0.26389e-04	0.12775e+00
u_i	0.11304e+02	0.33765e-04	0.22126e+01
$u_{i-2}u_{i-3}^2$	-0.23109e+01	0.36811e-04	0.83612e+00
$F_{i-2}F_{i-4}u_{i-3}$	-0.22816e+00	0.12014e-04	0.94324e-01
$F_{i-4}u_{i-1}$	0.67476e-02	0.13726e-04	0.27316e-02
$F_{i-3}F_{i-4}u_{i-3}$	0.95055e-01	0.47850e-05	0.48011e-01
$F_{i-1}F_{i-4}u_{i-3}$	0.89978e-05	0.55889e-05	0.52788e-01

Table 2: Parameter table for NARMAX model : $KC = 3.31$.

Model Term	Parameter	ERR	St.Dev.
F_{i-1}	0.12801e+01	0.99076e+00	0.97851e-01
F_{i-2}	-0.27820e+00	0.91281e-02	0.99927e-01
u_{i-3}^3	-0.58193e+00	0.29066e-04	0.10483e+00
F_{i-4}^3	-0.43380e-01	0.95587e-05	0.12795e-01
$F_{i-3}F_{i-4}^2$	0.41553e-01	0.28922e-05	0.12899e-01
u_i^3	0.47740e+00	0.16569e-04	0.14023e+00
$F_{i-4}u_iu_{i-1}$	-0.60782e-01	0.32752e-05	0.32026e-01

Table 3: Parameter table for NARMAX model : $KC = 6.48$.

Model Term	Parameter	ERR	St.Dev.
F_{i-1}	0.18021e+01	0.98490e+00	0.95162e-01
F_{i-2}	-0.78516e+00	0.14217e-01	0.14038e+00
F_{i-4}	-0.41016e-01	0.35150e-03	0.50713e-01
u_{i-3}^3	-0.41113e+00	0.46961e-04	0.45955e-01
u_i^3	0.92188e+00	0.30771e-04	0.11052e+00
$F_{i-1}u_i^2$	-0.31250e+00	0.69055e-04	0.53067e-01
$F_{i-4}u_{i-3}$	0.42653e+04	0.84596e-04	0.14323e+04
$F_{i-4}u_i$	0.84966e+04	0.52659e-04	0.28530e+04
$F_{i-1}F_{i-2}u_i$	0.33159e-01	0.33000e-04	0.10812e-01
$F_{i-4}u_{i-1}$	-0.12659e+05	0.29321e-04	0.42508e+04

Table 4: Parameter table for NARMAX model : $KC = 11.88$.

Model Term	Parameter	ERR	St.Dev.
F_{i-1}	0.16842e+01	0.99554e+00	0.68816e-01
F_{i-2}	-0.64108e+00	0.42679e-02	0.66371e-01
F_{i-1}^3	-0.26385e-01	0.18700e-04	0.72448e-02
u_i	-0.80901e-01	0.70946e-05	0.29273e+00
u_{i-2}	-0.94940e-01	0.22122e-04	0.24563e+00
u_i^3	0.83598e+00	0.24634e-04	0.13375e+00
$F_{i-3}u_{i-3}^2$	-0.58117e+00	0.10666e-04	0.11554e+00
$F_{i-2}F_{i-4}u_{i-3}$	0.14757e+00	0.16333e-04	0.34883e-01

Table 5: Parameter table for NARMAX model : $KC = 17.5$.

Model Term	Parameter	ERR	St.Dev.
F_{i-1}	0.16968e+01	0.98733e+00	0.10319e+00
F_{i-2}	-0.92220e+00	0.10677e-01	0.19801e+00
F_{i-1}^3	0.62466e-01	0.34870e-03	0.26433e-01
u_{i-3}^3	-0.58983e+00	0.13139e-03	0.89619e-01
u_i^3	0.15208e+01	0.35151e-03	0.34248e+00
$F_{i-1}u_i^2$	-0.80145e+00	0.21335e-03	0.22362e+00
F_{i-4}^2	0.46783e-02	0.53122e-04	0.26860e-02
F_{i-3}	0.22397e+00	0.36680e-04	0.11904e+00
u_{i-3}	-0.33093e-01	0.18081e-04	0.29828e-01

Table 6: Parameter table for NARMAX model : $KC = 34.68$.

KC	MSE	$\frac{MSE}{MSE(Morison)}$
3.31	0.011	0.228
6.48	0.005	0.018
11.88	0.018	0.003
17.50	0.009	0.017
34.68	0.084	0.056

Table 7: MSE values for OLS fit to U-tube data.

$f_s(Hz)$	MSE
20.0	2.172
10.0	2.256
5.0	2.339

Table 8: MSE values for discrete Morison fit to OA1F1 data.

Decimation Factor	Model Term	Parameter	ERR	St.Dev.
1	u_i	0.34616e+04	0.41756e-01	0.16720e+02
	u_{i-1}	-0.34434e+04	0.93366e+00	0.16652e+02
	u_i^3	0.61468e+02	0.28627e-02	0.53679e+01
2	u_i	0.17843e+04	0.93047e+00	0.88072e+01
	u_{i-1}	-0.17777e+04	0.16854e-01	0.87101e+01
	u_i^3	0.75793e+02	0.30123e-01	0.58492e+01
4	u_i	0.89092e+03	0.23972e-01	0.46741e+01
	u_{i-1}	-0.89878e+03	0.94932e+00	0.44681e+01
	u_i^3	0.81435e+02	0.33366e-02	0.68324e+01

Table 9: Parameter tables for Morison models of OA1F1 data.

$f_s(Hz)$	MSE	$\frac{MSE}{MSE(Morison)}$
20.0	0.241	0.111
10.0	0.675	0.299
5.0	1.246	0.533

Table 10: MSE values for OLS analysis of OA1F1 data.

Decimation Factor	Model Term	Parameter	ERR	St.Dev.
1	F_{i-1}	0.10527e+01	0.99339e+00	0.15631e-01
	F_{i-4}	-0.24170e+00	0.32234e-02	0.12455e-01
	u_{i-4}	-0.19254e+03	0.20740e-03	0.12037e+02
	u_i	0.18877e+03	0.29104e-03	0.12110e+02
	u_{i-4}^3	0.19028e+02	0.10240e-03	0.21628e+01
	$F_{i-1}^2 u_{i-4}$	0.83766e-02	0.90080e-04	0.73806e-03
	$F_{i-1}F_{i-2}F_{i-4}$	-0.77932e-02	0.28166e-03	0.72594e-03
2	F_{i-1}	0.85124e+00	0.97386e+00	0.21853e-01
	F_{i-3}	-0.29028e+00	0.14644e-01	0.20183e-01
	u_{i-4}	-0.25433e+02	0.92557e-03	0.18812e+02
	u_i	0.73679e+03	0.13187e-02	0.40688e+02
	u_{i-1}	-0.71581e+03	0.14840e-02	0.53778e+02
	u_{i-4}^3	0.47754e+02	0.71568e-03	0.40493e+01
	$F_{i-1}^2 u_{i-4}$	0.10364e-02	0.30643e-03	0.15470e-03
4	F_{i-1}	0.48637e+00	0.91320e+00	0.29916e-01
	F_{i-4}	-0.24531e+00	0.53489e-01	0.22727e-01
	u_{i-4}	0.15107e+02	0.21704e-02	0.12213e+02
	u_i	0.74223e+03	0.38881e-02	0.22395e+02
	u_{i-1}	-0.75752e+03	0.10346e-01	0.29543e+02
	u_{i-3}^3	0.85848e+02	0.22339e-02	0.60891e+01
	$F_{i-3}F_{i-5}^2$	0.62316e-05	0.78293e-03	0.77790e-06
	F_{i-2}	-0.34339e+00	0.58334e-03	0.34145e-01
	F_{i-3}	0.27752e+00	0.84541e-03	0.33932e-01

Table 11: Parameter tables for NARMAX models of OA1F1 data.

Model Term	Parameter	ERR	St.Dev.
u_i	0.88080e+03	0.18764e-01	0.20344e+02
u_{i-1}	-0.84593e+03	0.38539e+00	0.20008e+02
u_i^3	0.33983e+02	0.38132e+00	0.21913e+01

Table 12: Parameter table for Morison model of Christchurch Bay data.

Model Term	Parameter	*ERR*	St.Dev.
F_{i-1}	0.18615e+01	0.95655e+00	0.70177e-01
F_{i-2}	-0.11551e+01	0.29096e-01	0.13558e+00
F_{i-1}^3	-0.66218e-05	0.76435e-03	0.41434e-05
$F_{i-1}^2 F_{i-4}$	-0.36266e-06	0.90966e-03	0.61313e-06
$F_{i-1} u_{i-4}^2$	-0.21047e+00	0.43745e-03	0.28399e-01
$F_{i-4} u_i^2$	0.19212e+00	0.51797e-03	0.18074e-01
$F_{i-3} u_i u_{i-4}$	-0.42832e+00	0.55750e-03	0.33347e-01
$F_{i-2} u_{i-3}^2$	0.42050e+00	0.69171e-03	0.47320e-01
F_{i-3}^2	-0.20219e-03	0.34152e-03	0.55597e-04
$F_{i-2} F_{i-5}$	0.14279e-03	0.27665e-03	0.70706e-04
$F_{i-1} F_{i-2} u_i$	-0.79306e-03	0.10157e-03	0.10556e-03
$F_{i-1}^2 u_{i-4}$	0.48154e-03	0.14678e-03	0.58257e-04
$u_{i-3} u_{i-4}^2$	0.50511e+02	0.23129e-03	0.14101e+02
$u_i u_{i-4}^2$	0.18365e+03	0.10878e-03	0.29600e+02
$u_{i-1} u_{i-4}^2$	-0.22708e+03	0.50493e-03	0.42018e+02
F_{i-2}^3	0.13557e-04	0.74931e-04	0.42904e-05
$F_{i-1} F_{i-2}^2$	-0.32915e-04	0.19974e-03	0.12754e-04
$F_{i-1}^2 F_{i-3}$	0.24301e-05	0.11394e-03	0.10739e-05
$F_{i-1}^2 F_{i-2}$	0.24703e-04	0.23297e-04	0.12493e-04
F_{i-5}	-0.36463e+00	0.16677e-04	0.10016e+00
F_{i-4}	0.14370e+00	0.37472e-04	0.11225e+00
F_{i-6}	0.14133e+00	0.43328e-04	0.46771e-01
u_i	0.11428e+03	0.93507e-05	0.37205e+02
u_{i-1}	-0.24760e+03	0.76597e-04	0.10773e+03
u_{i-2}	0.20084e+03	0.31621e-04	0.15248e+03
F_{i-3}	0.28620e+00	0.35747e-04	0.13075e+00
u_{i-3}	-0.44304e+02	0.11110e-04	0.15693e+03
u_{i-5}	0.27294e+02	0.78658e-05	0.36969e+02
u_{i-4}	-0.46985e+02	0.13122e-05	0.11163e+03

Table 13: Parameter table for NARMAX model of Christchurch Bay data.

Data : Velocity

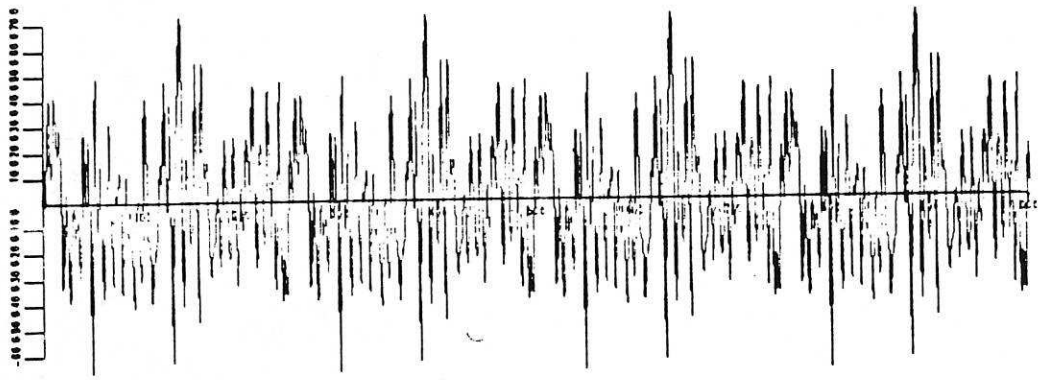

Data : Force

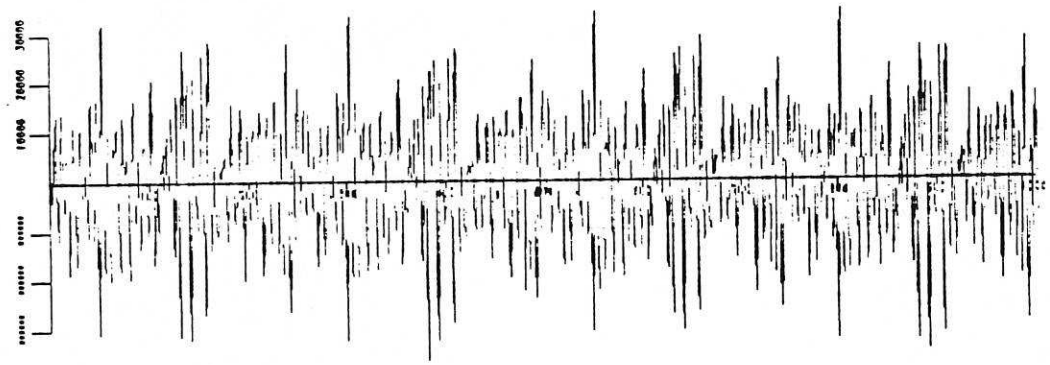

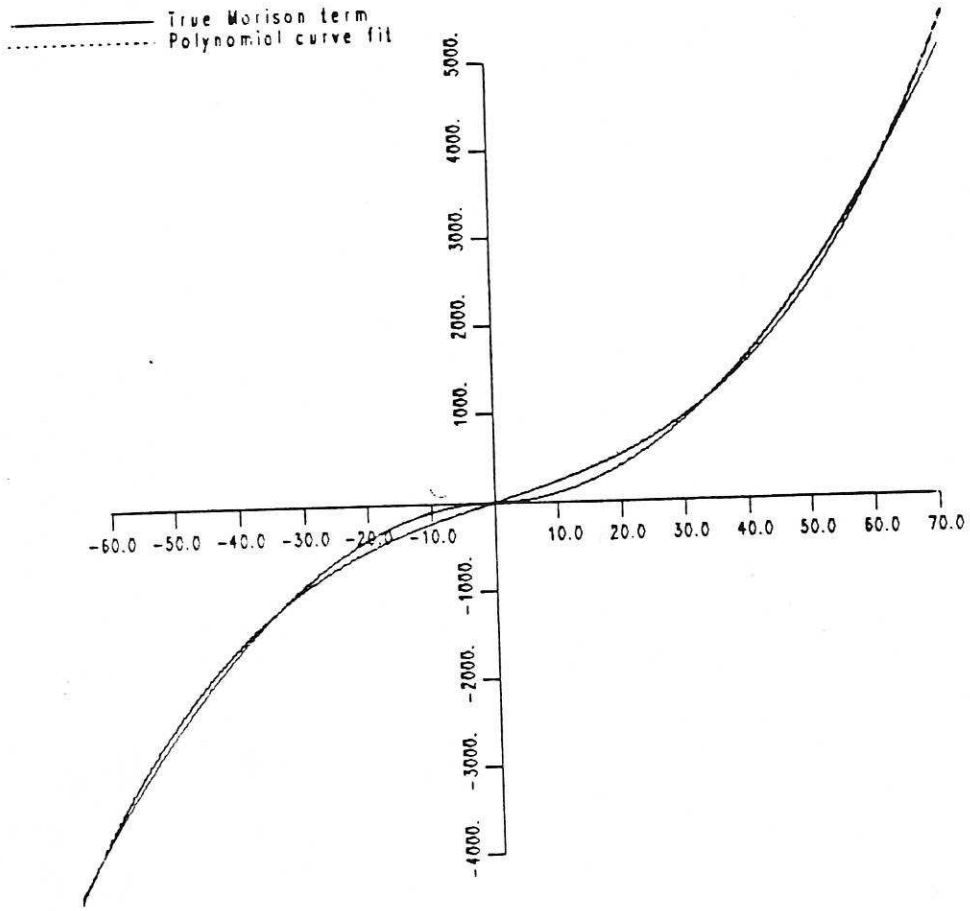
True Morison term
Polynomial curve fit
5000.
4000.
3000.
2000.
1000.
-1000.
-2000.
-3000.
-4000.
-60.0
-50.0
-40.0
-30.0
-20.0
-10.0
10.0
20.0
30.0
40.0
50.0
60.0
70.0

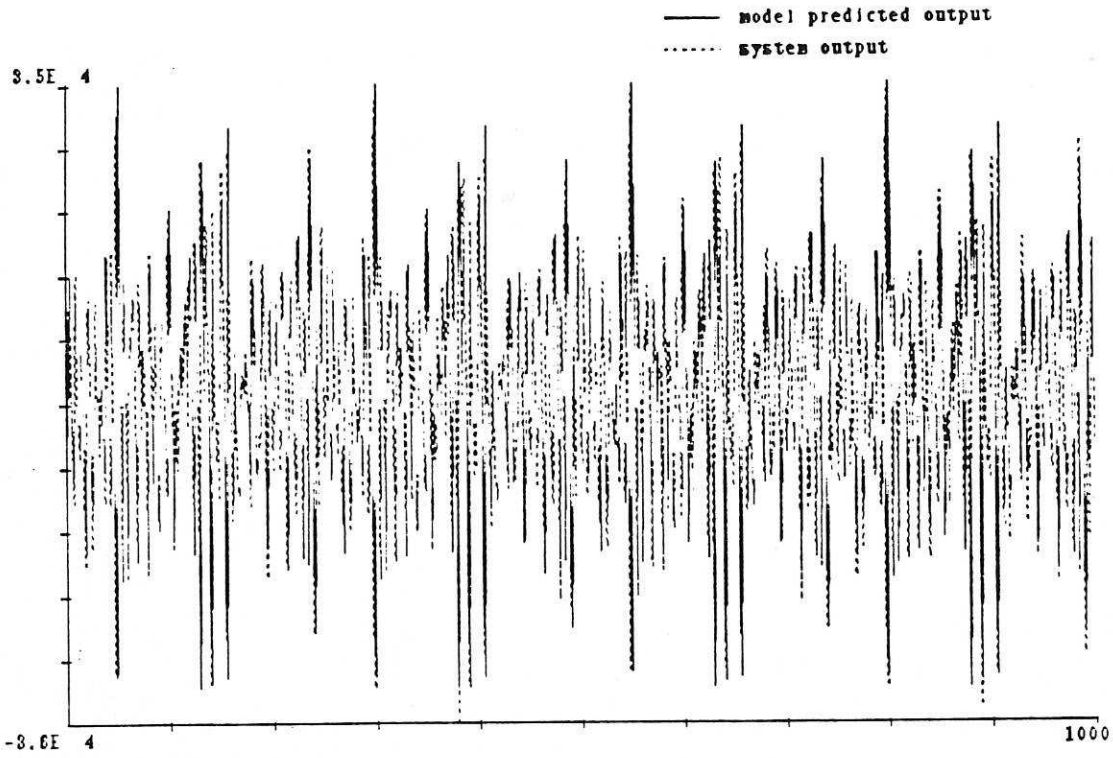
model predicted output
system output
8.5E 4
-8.0E 4
1000

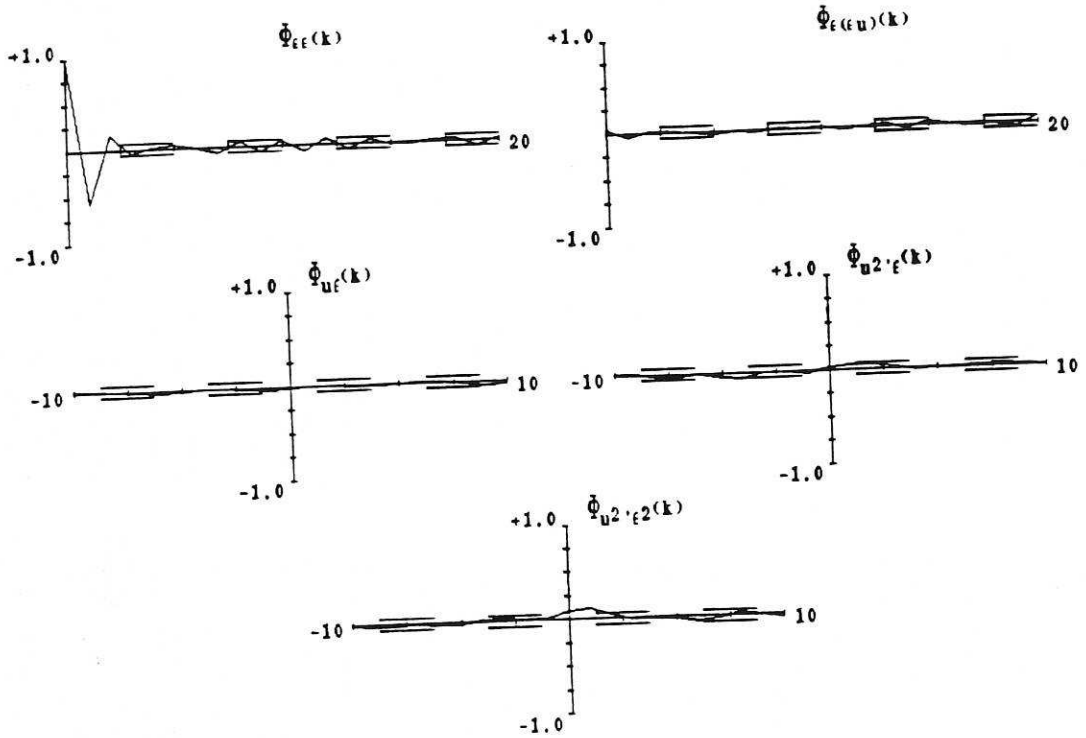
$\Phi_{\varepsilon\varepsilon}(k)$
+1.0
-1.0
20
$\Phi_{\varepsilon(\varepsilon u)}(k)$
+1.0
-1.0
20
$\Phi_{uf}(k)$
+1.0
-1.0
-10
10
$\Phi_{u2\cdot\varepsilon}(k)$
+1.0
-1.0
-10
10
$\Phi_{u2\cdot\varepsilon 2}(k)$
+1.0
-1.0
-10
10

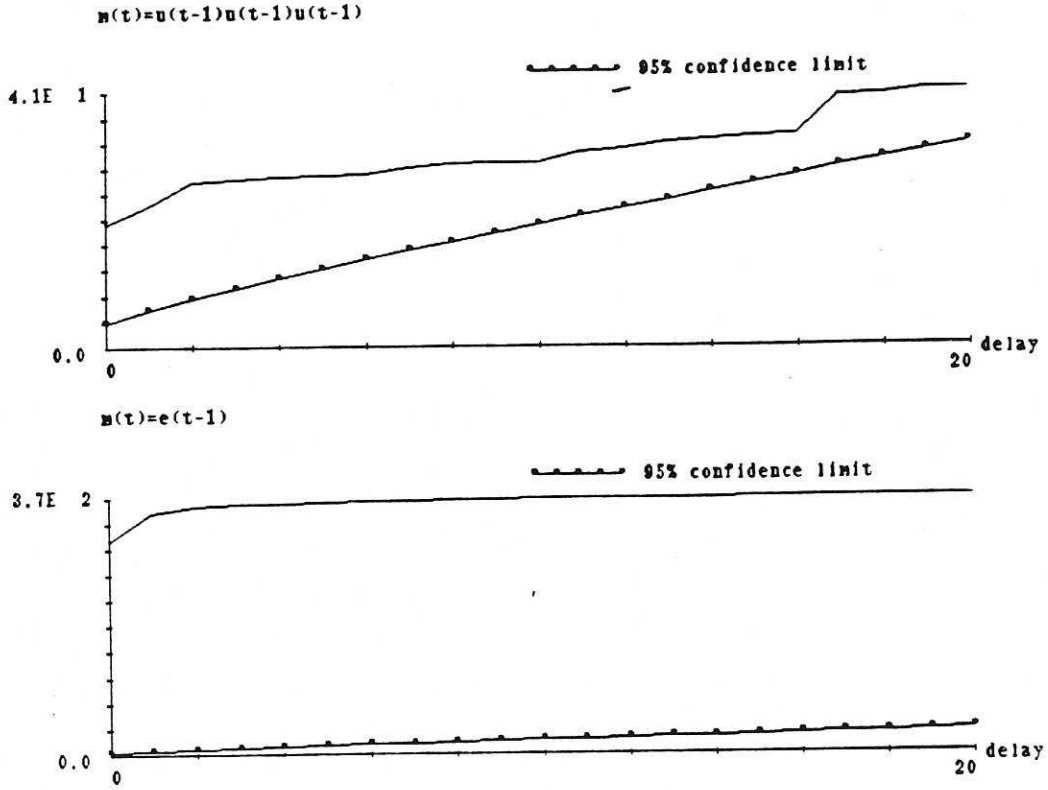
n(t)=u(t-1)u(t-1)u(t-1)
95% confidence limit
4.1E 1
0.0
0
20
delay
n(t)=e(t-1)
95% confidence limit
3.7E 2
0.0
0
20
delay

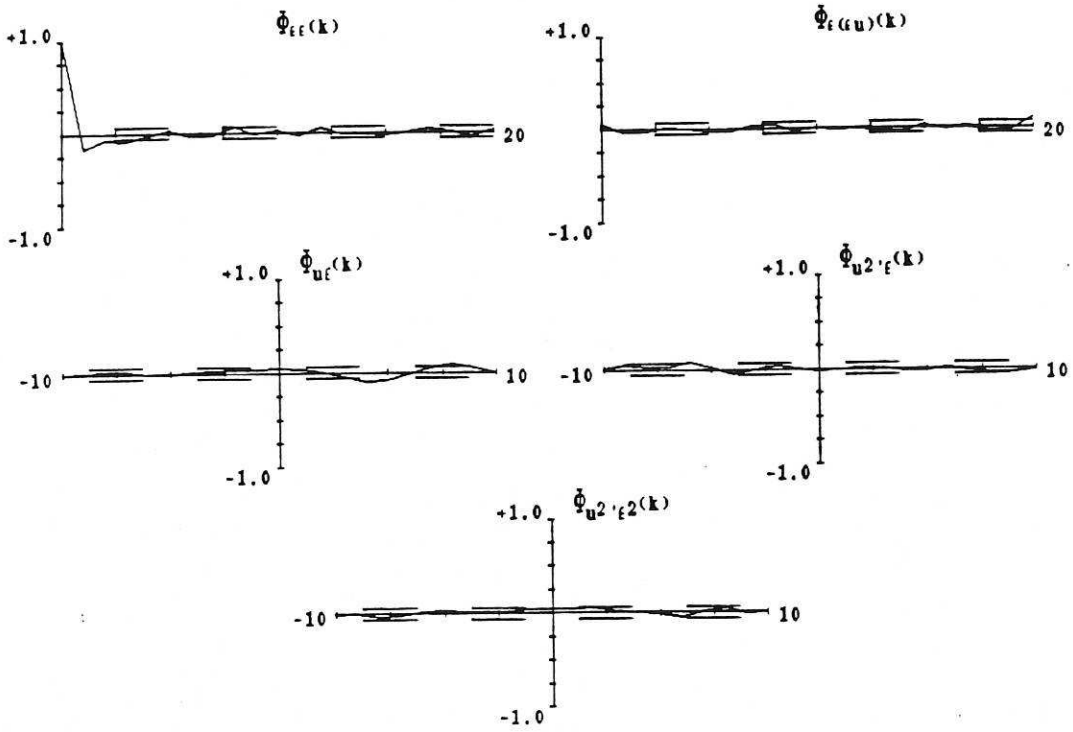
$\Phi_{\varepsilon\varepsilon}(k)$
+1.0
-1.0
20
$\Phi_{\varepsilon(\Delta u)}(k)$
+1.0
-1.0
20
$\Phi_{u\varepsilon}(k)$
+1.0
-1.0
-10
10
$\Phi_{u2,\varepsilon}(k)$
+1.0
-1.0
-10
10
$\Phi_{u2,\varepsilon2}(k)$
+1.0
-1.0
-10
10

a)

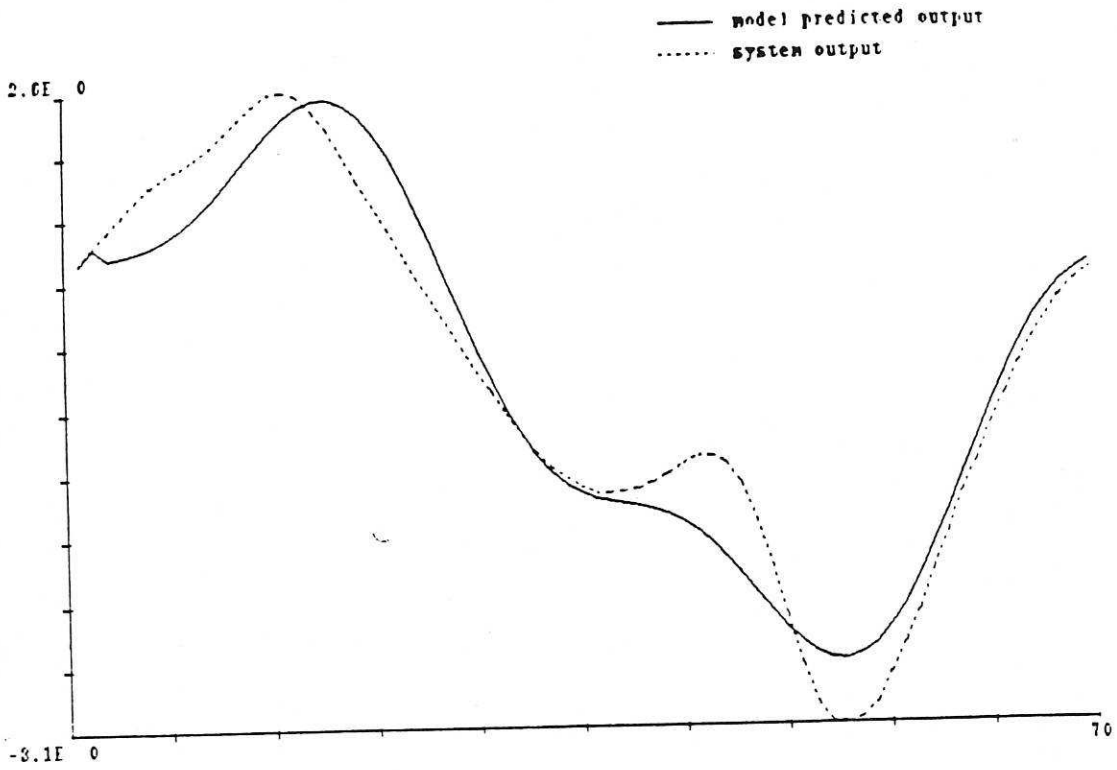
model predicted output
system output
2.0E 0
-3.1E 0
70

b)

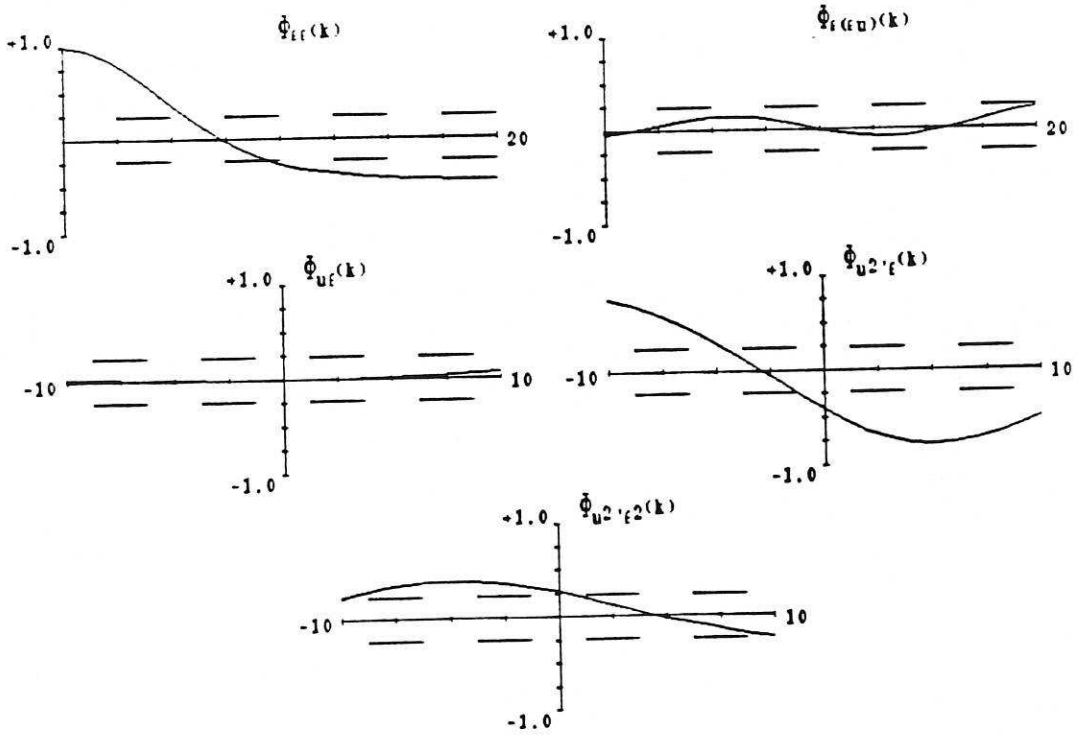
$\Phi_{ff}(k)$
+1.0
-1.0
20
$\Phi_{f(fu)}(k)$
+1.0
-1.0
20
$\Phi_{uf}(k)$
+1.0
-1.0
-10
10
$\Phi_{u^2 f}(k)$
+1.0
-1.0
-10
10
$\Phi_{u^2 f^2}(k)$
+1.0
-1.0
-10
10

a)

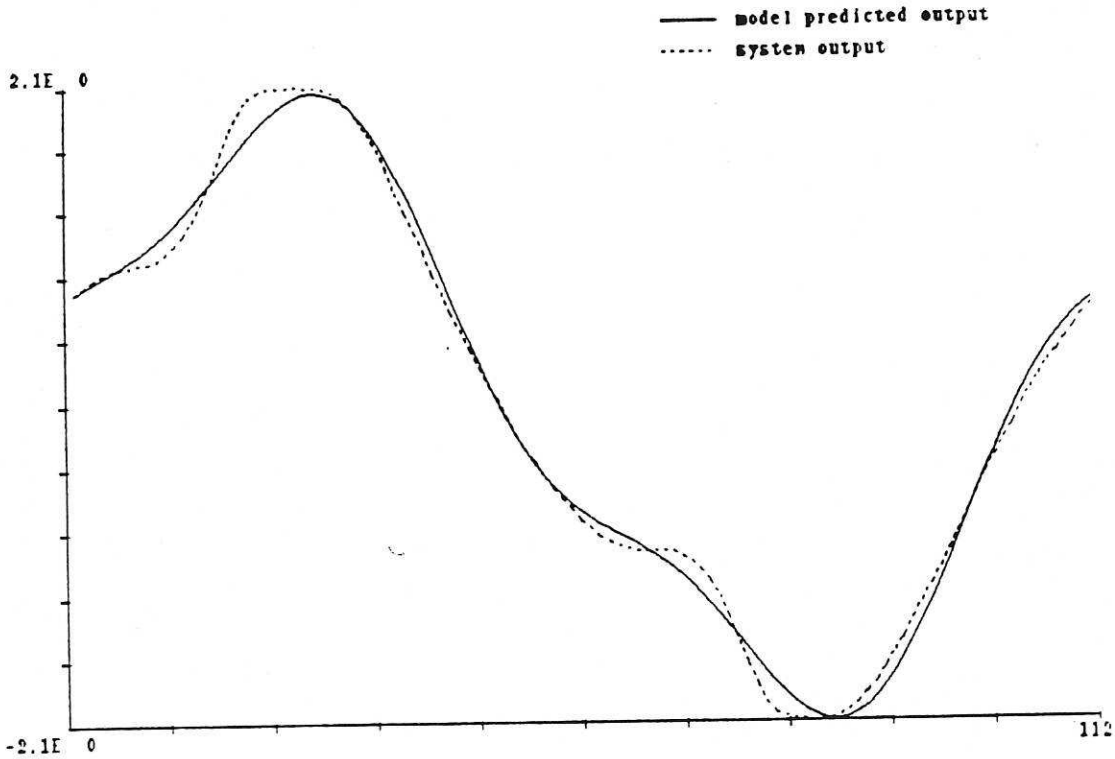
model predicted output
system output
2.1E 0
-2.1E 0
112

b)

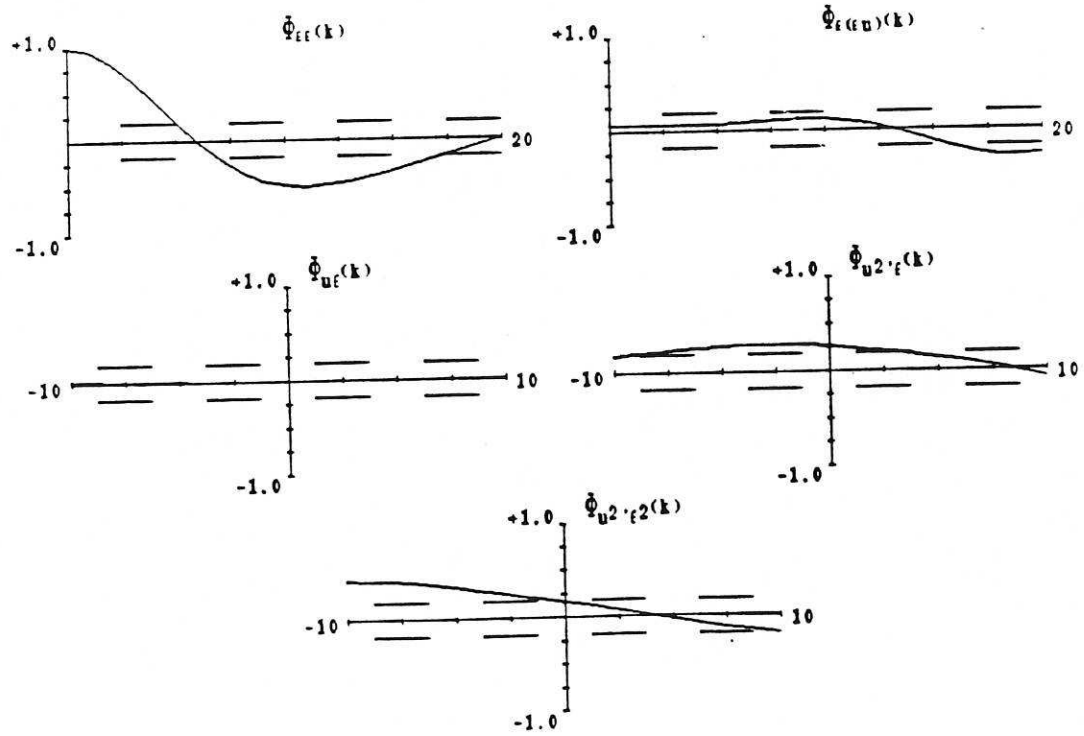
$\Phi_{ff}(k)$
+1.0
-1.0
20
$\Phi_{f(fu)}(k)$
+1.0
-1.0
20
$\Phi_{uf}(k)$
+1.0
-1.0
-10
10
$\Phi_{u2'f}(k)$
+1.0
-1.0
-10
10
$\Phi_{u2'f2}(k)$
+1.0
-1.0
-10
10

a)

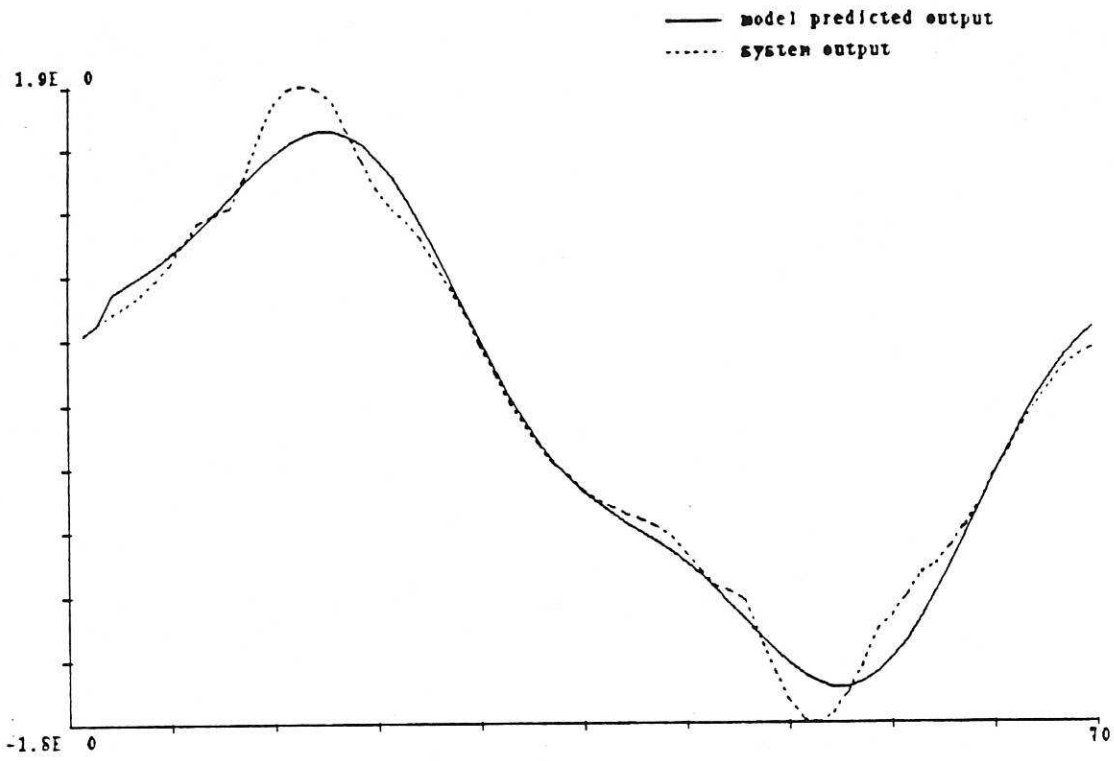
model predicted output
system output
1.9E 0
-1.8E 0
70

b)

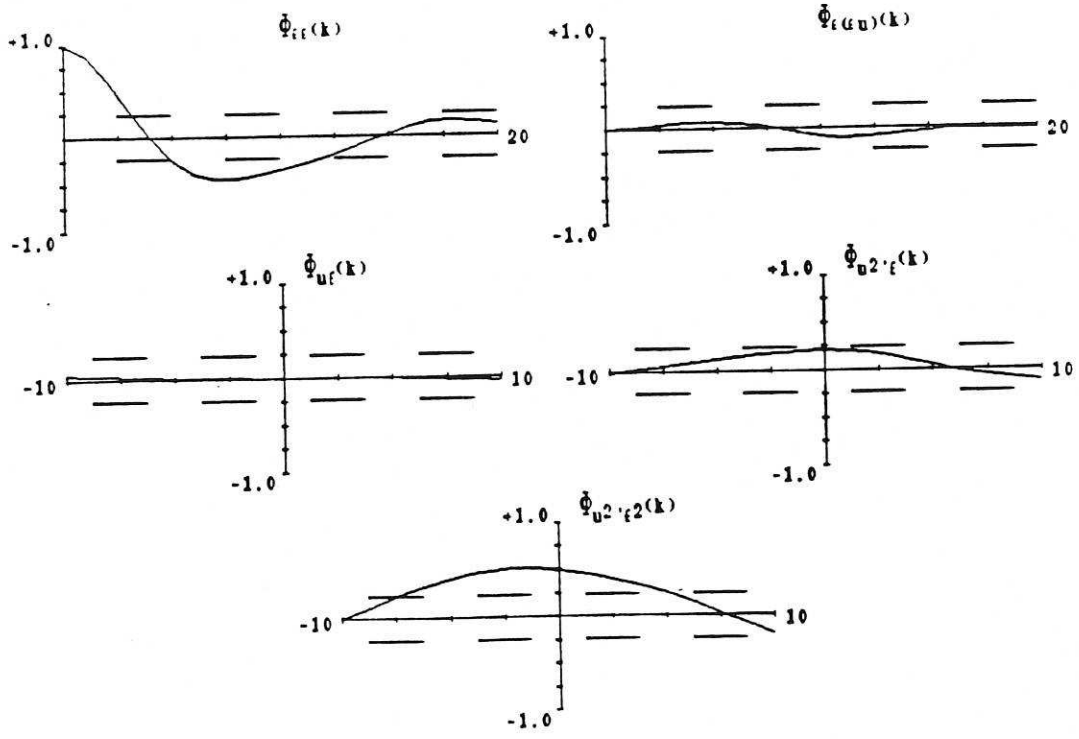
$\Phi_{ff}(k)$
$\Phi_{f(u)}(k)$
$\Phi_{uf}(k)$
$\Phi_{u^2 f}(k)$
$\Phi_{u^2 f^2}(k)$
+1.0
-1.0
20
10
-10

a)

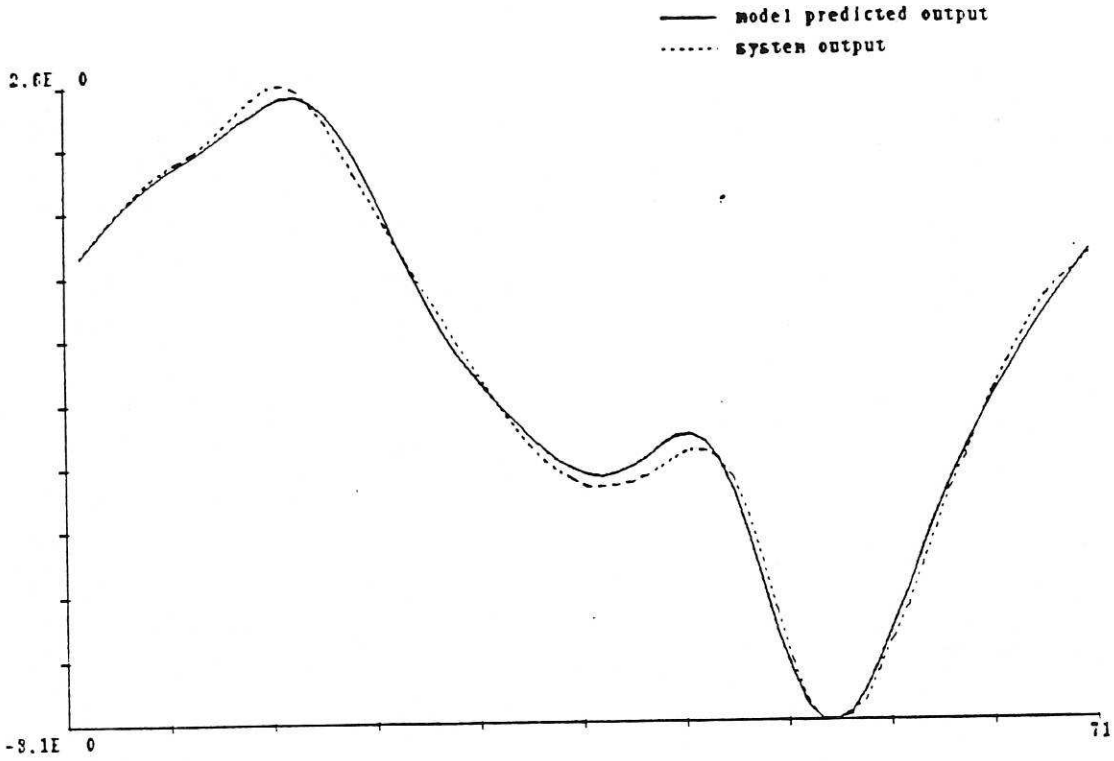
model predicted output
system output
2.6E 0
-8.1E 0
71

b)

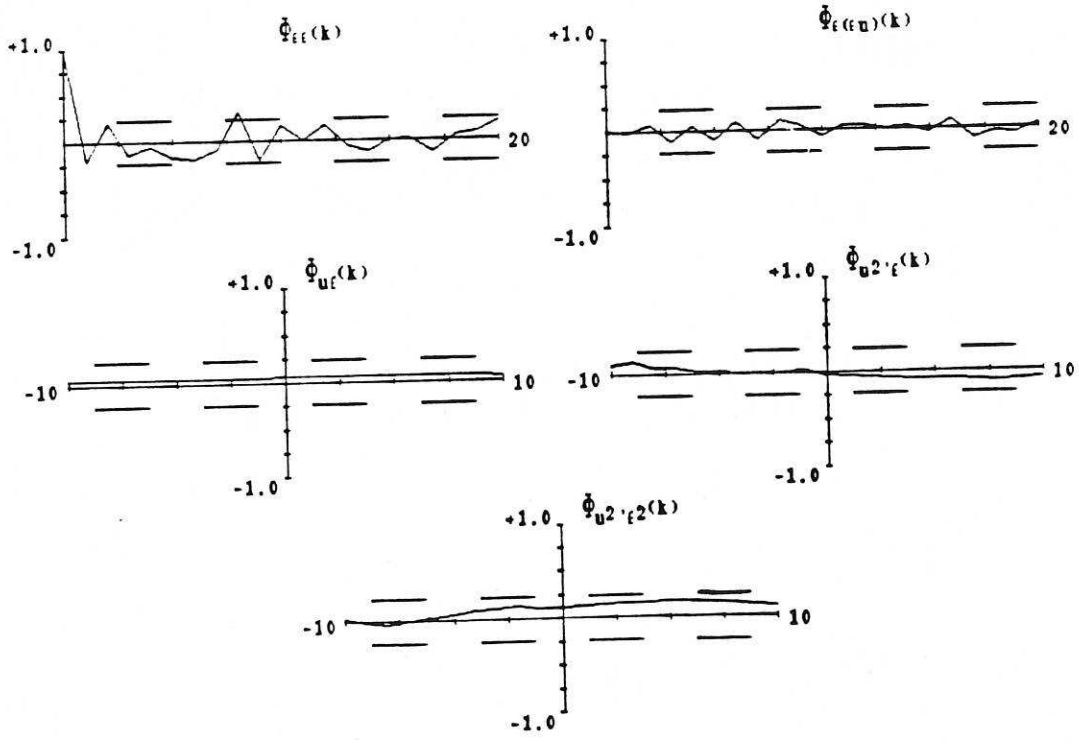
$\Phi_{ff}(k)$
$\Phi_{f(fu)}(k)$
$\Phi_{uf}(k)$
$\Phi_{u^2 f}(k)$
$\Phi_{u^2 f^2}(k)$
+1.0
-1.0
20
10
-10

a)

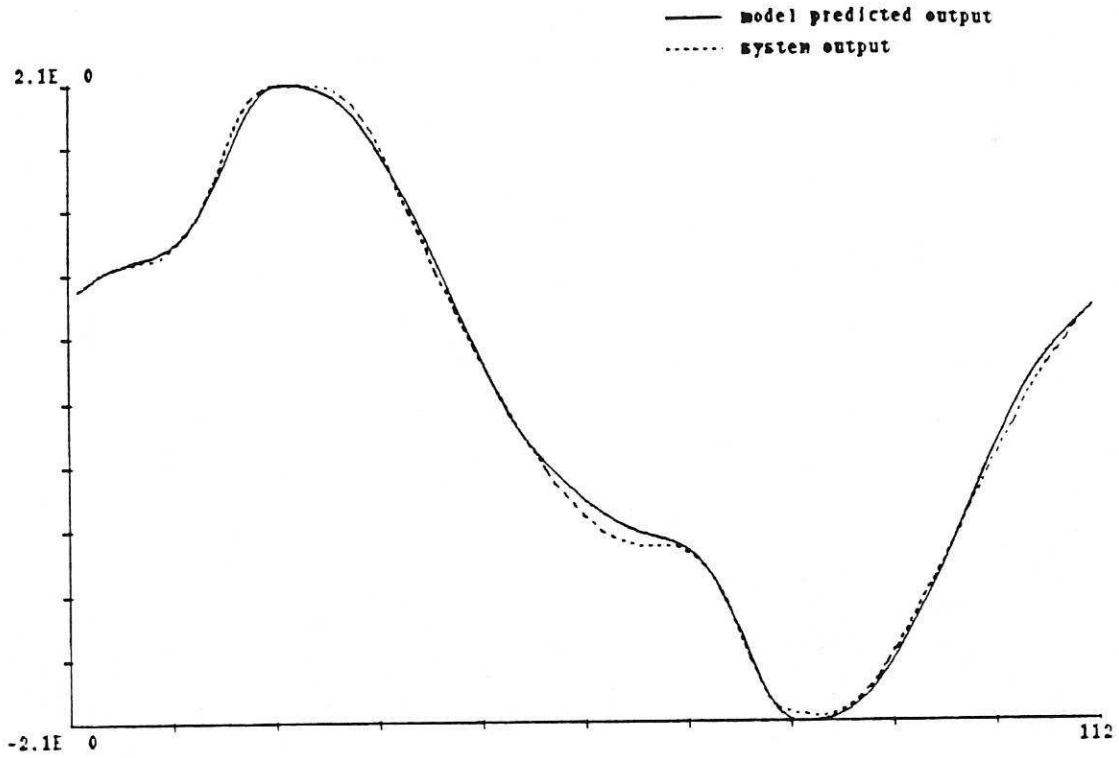
model predicted output
system output
2.1E 0
-2.1E 0
112

b)

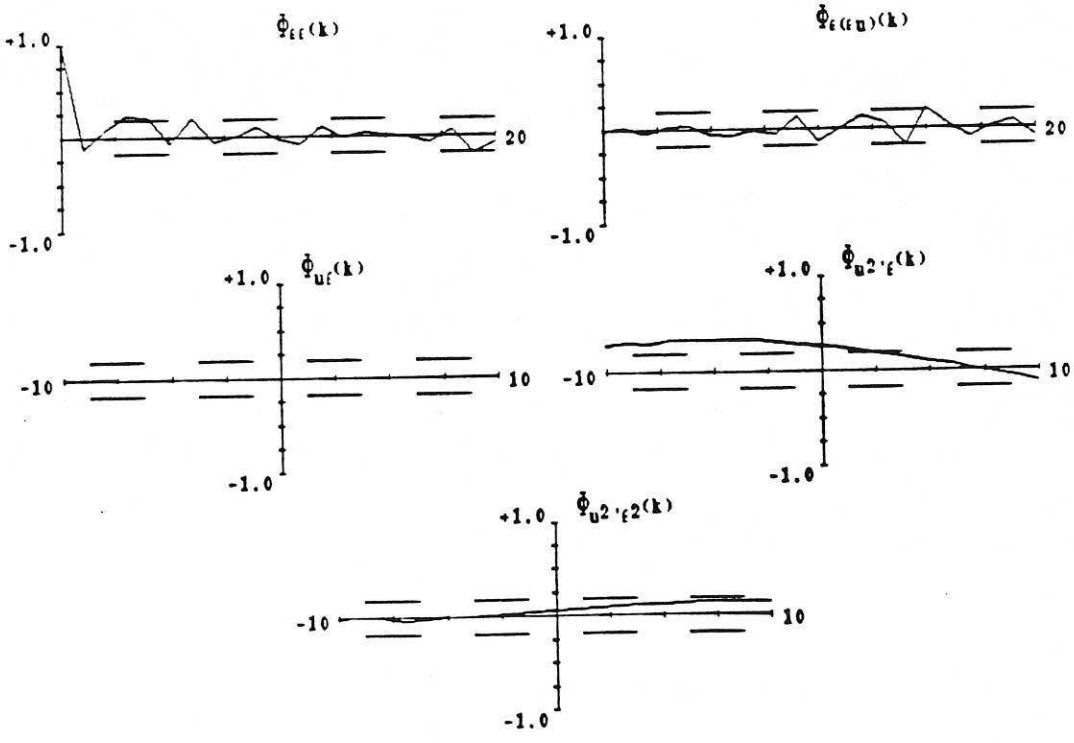
$\Phi_{ff}(k)$
+1.0
-1.0
20
$\Phi_{f(fu)}(k)$
+1.0
-1.0
20
$\Phi_{uf}(k)$
+1.0
-1.0
-10
10
$\Phi_{u^2 f}(k)$
+1.0
-1.0
-10
10
$\Phi_{u^2 f^2}(k)$
+1.0
-1.0
-10
10

a)

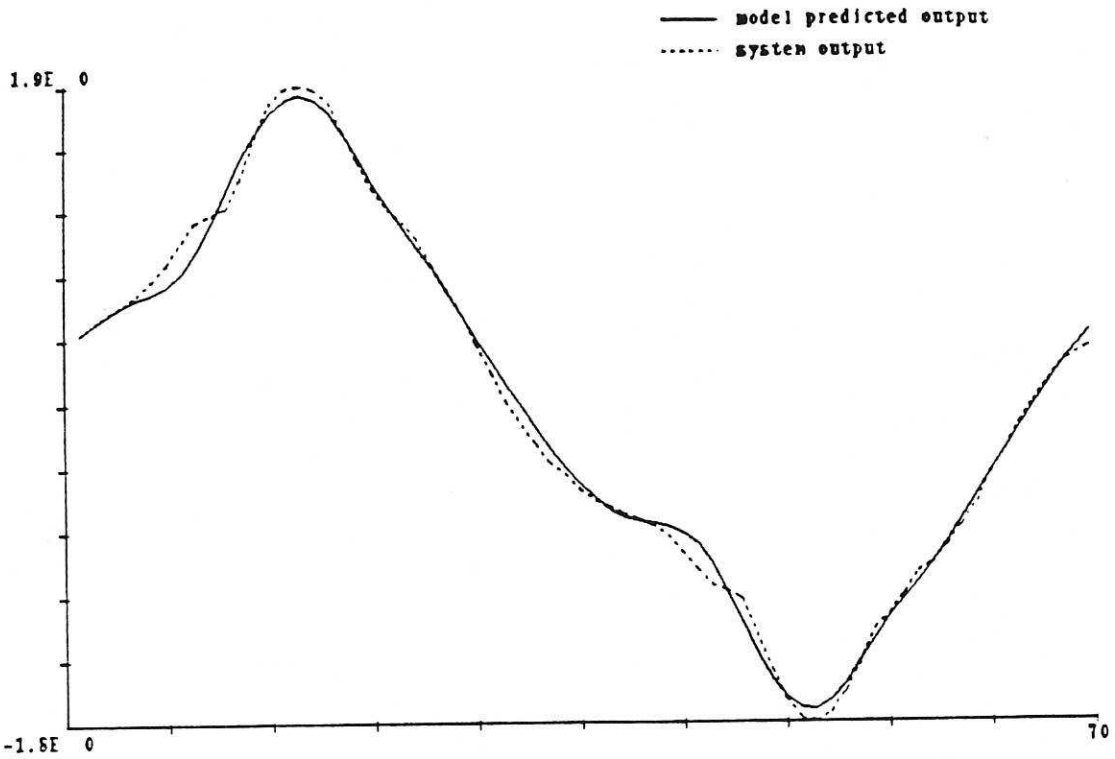

b)

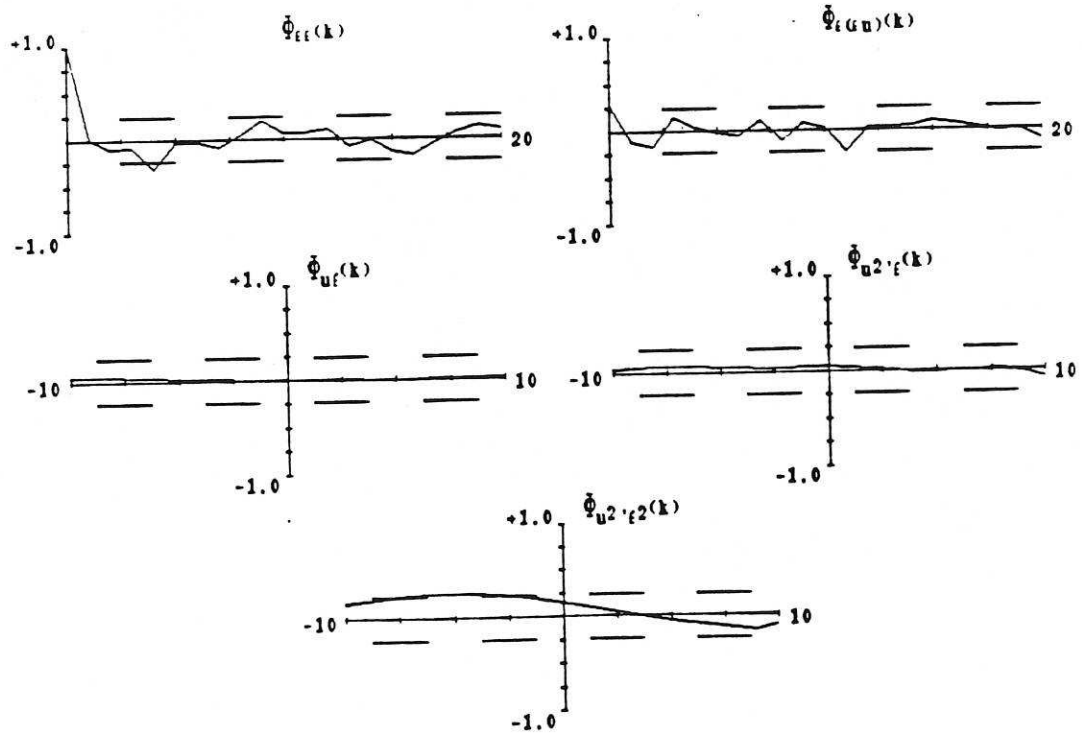

Velocity PSD

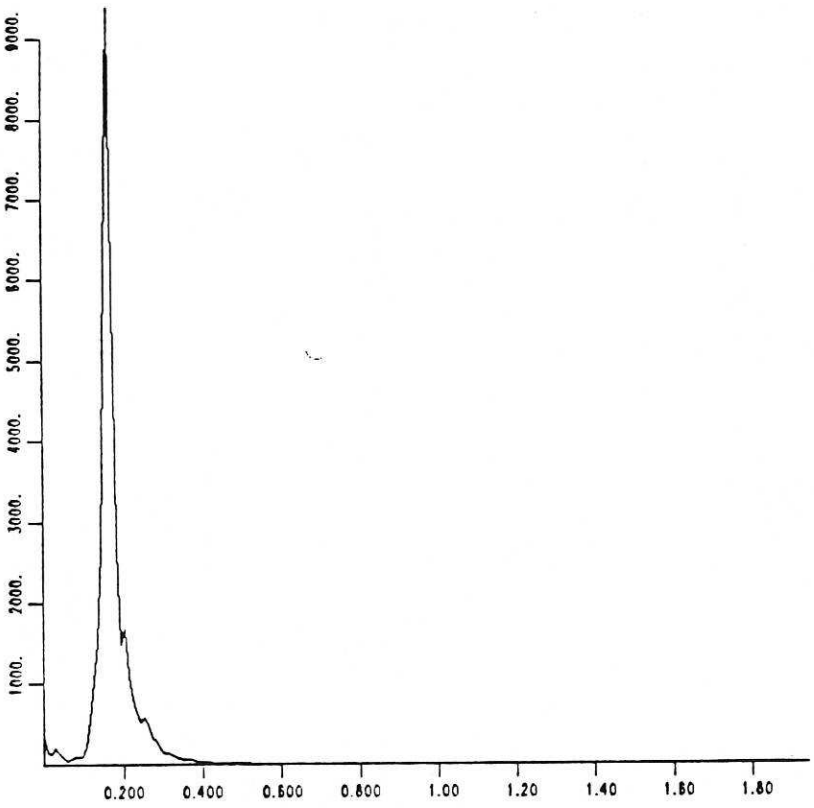

a)

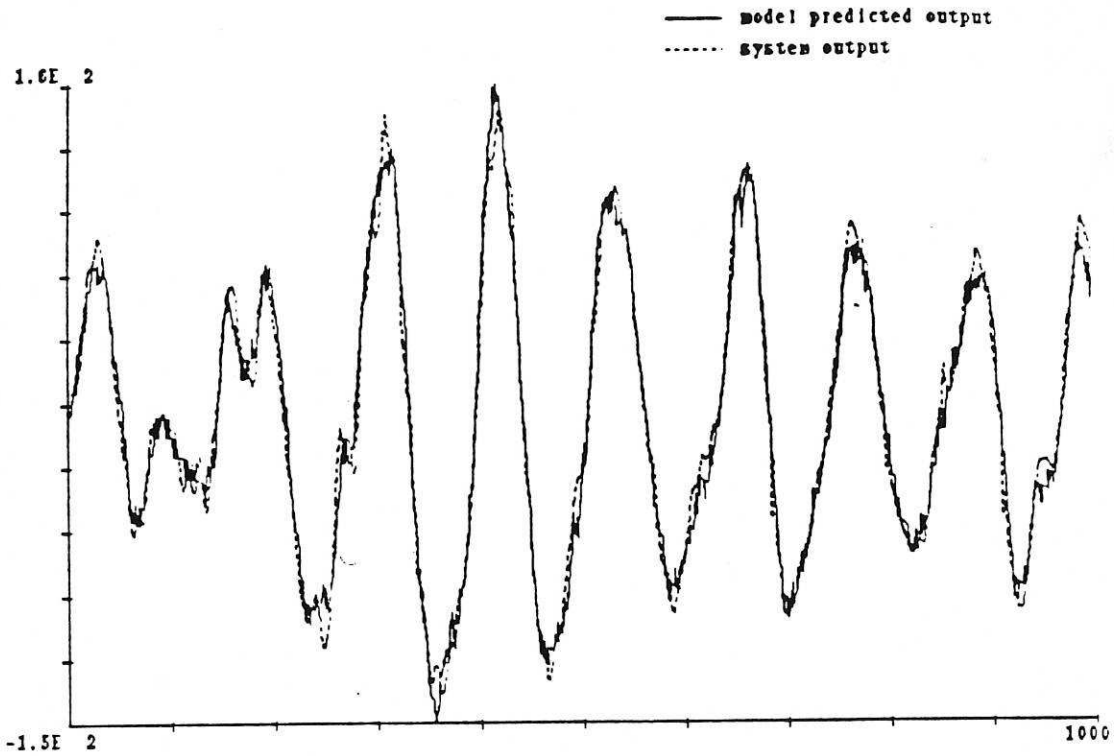
model predicted output
system output
1.6E 2
-1.5E 2
1000

b)

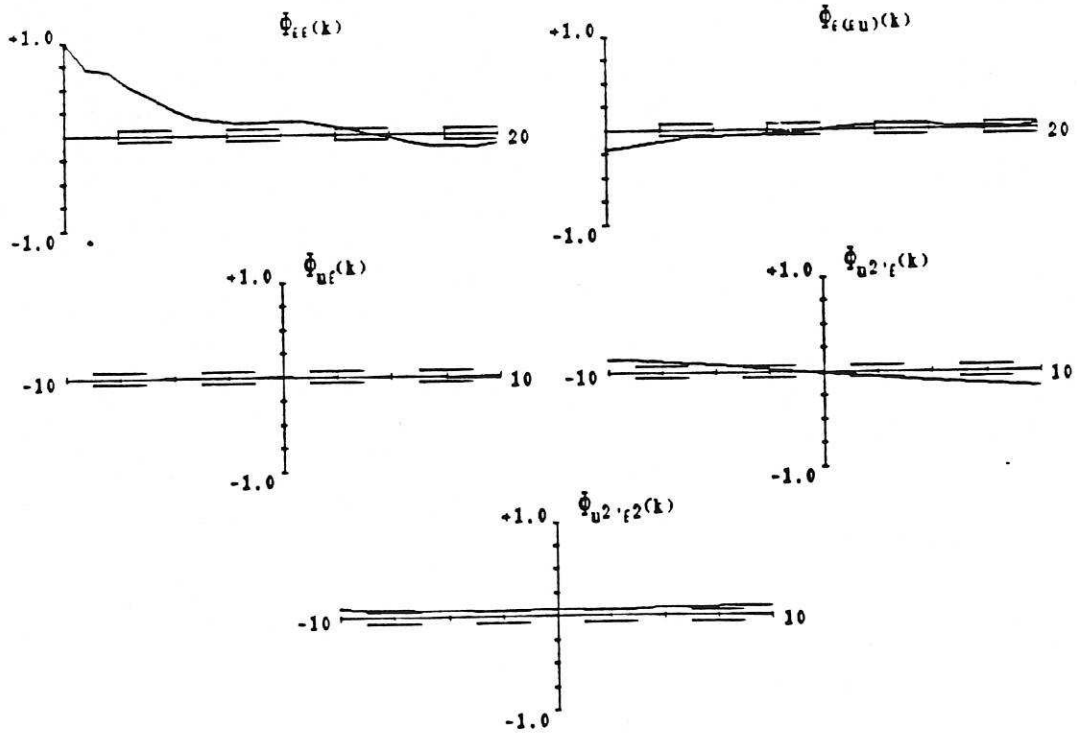
$\Phi_{ff}(k)$
+1.0
-1.0
20
$\Phi_{f(u)}(k)$
+1.0
-1.0
20
$\Phi_{uf}(k)$
+1.0
-1.0
-10
10
$\Phi_{u^2f}(k)$
+1.0
-1.0
-10
10
$\Phi_{u^2f^2}(k)$
+1.0
-1.0
-10
10

a)

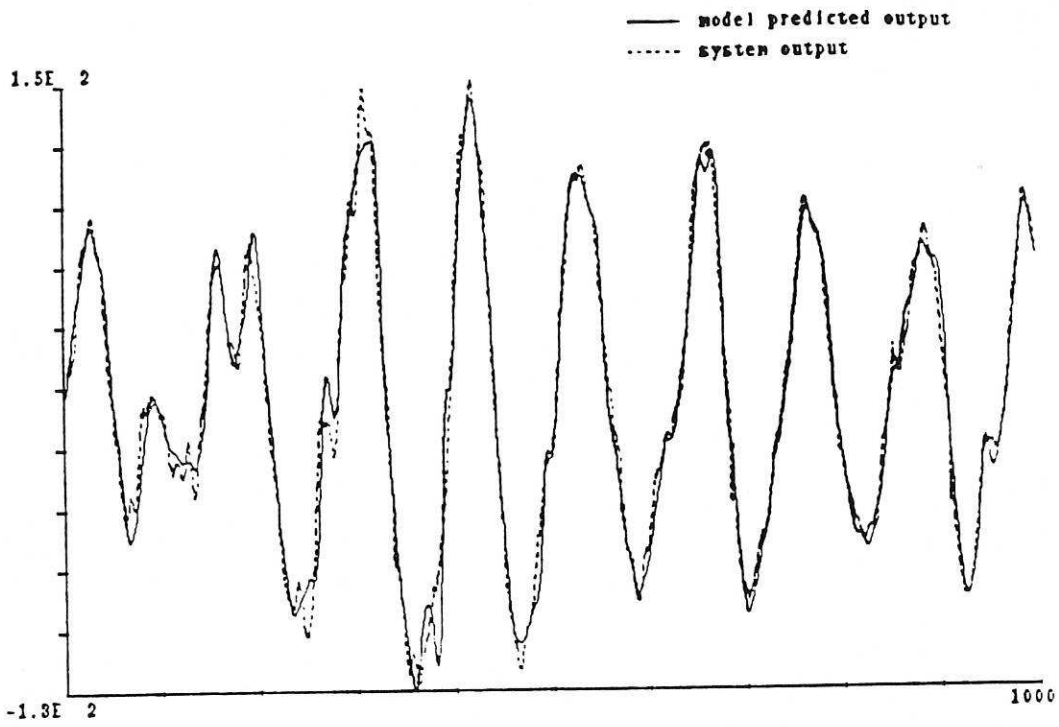
model predicted output
system output
1.5E 2
-1.3E 2
1000

b)

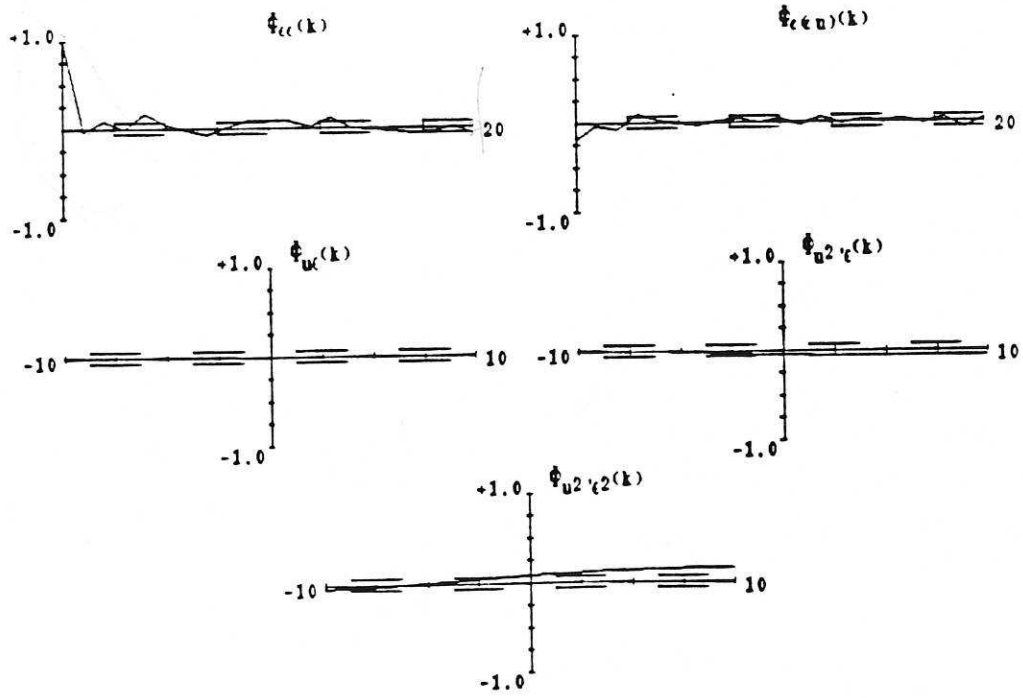
+1.0
-1.0
20
10
-10

File : sc_run_53_level_3
Data : Velocity - X component

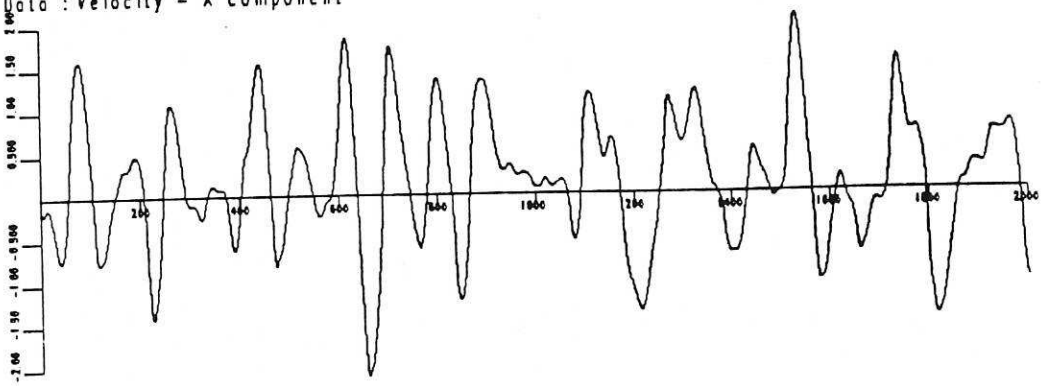

File : sc_run_53_level_3
Data : Velocity - Y component

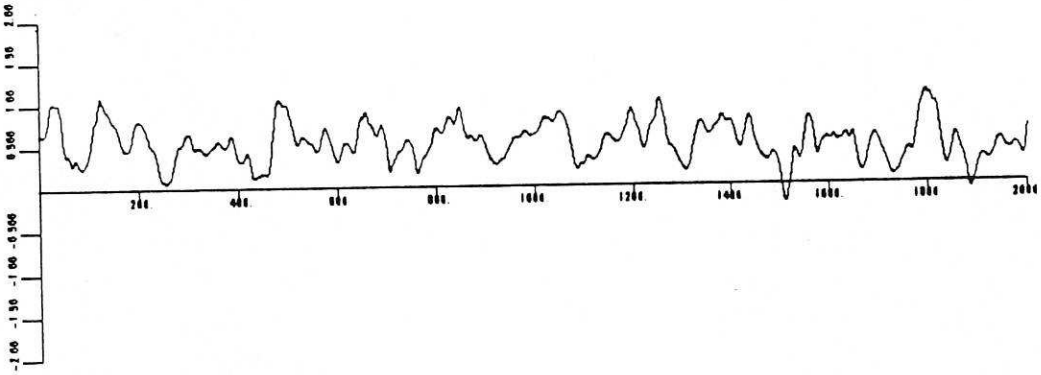

File : sc_run_53_level_3
Data : Velocity - Inline component

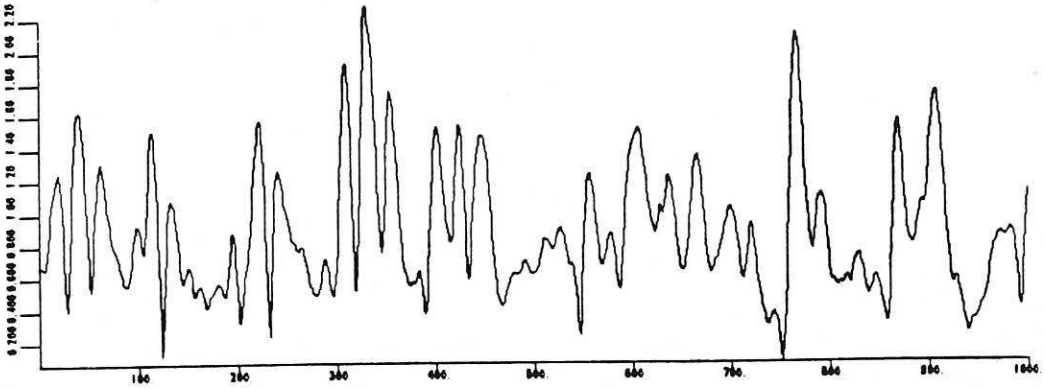

File : sc_run_53_level_3
Data : Velocity-X Angle

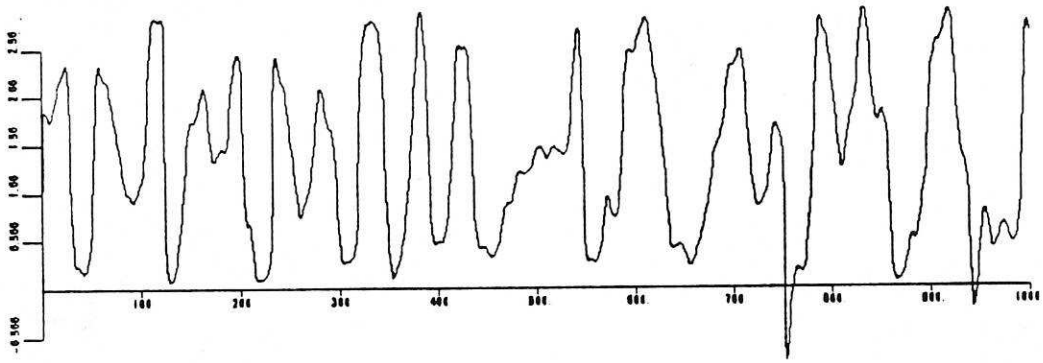

a)

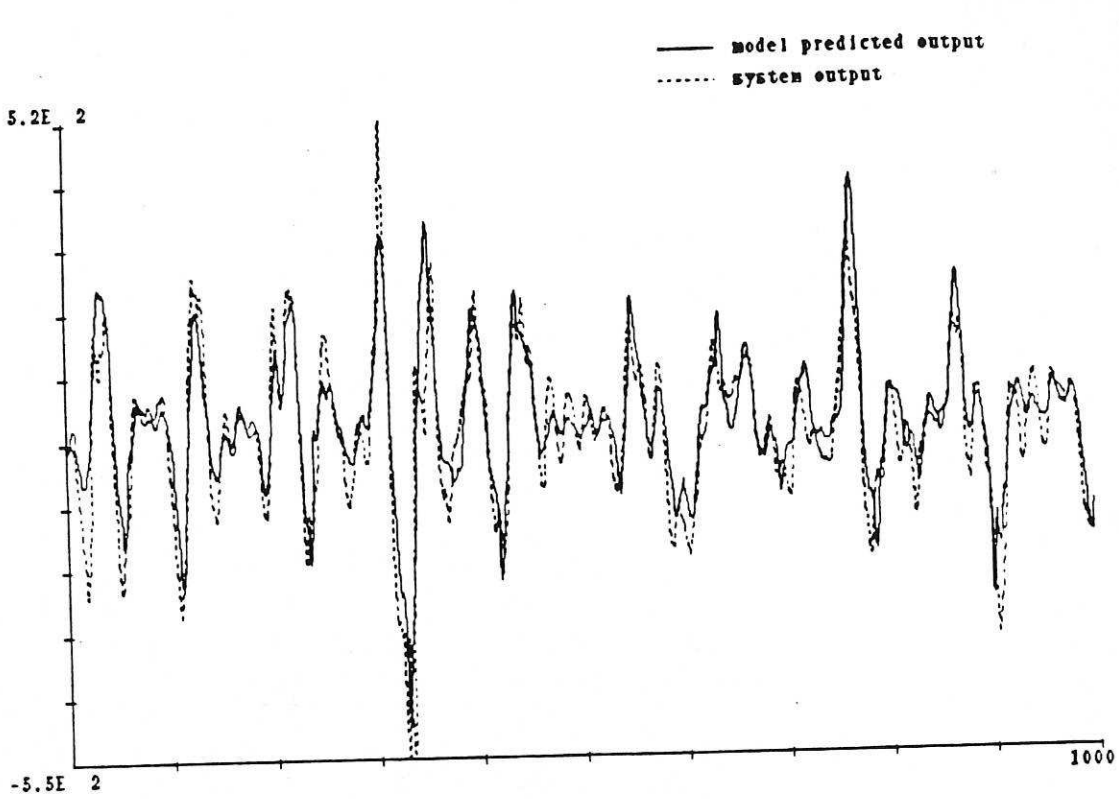
model predicted output
system output
5.2E 2
-5.5E 2
1000

b)

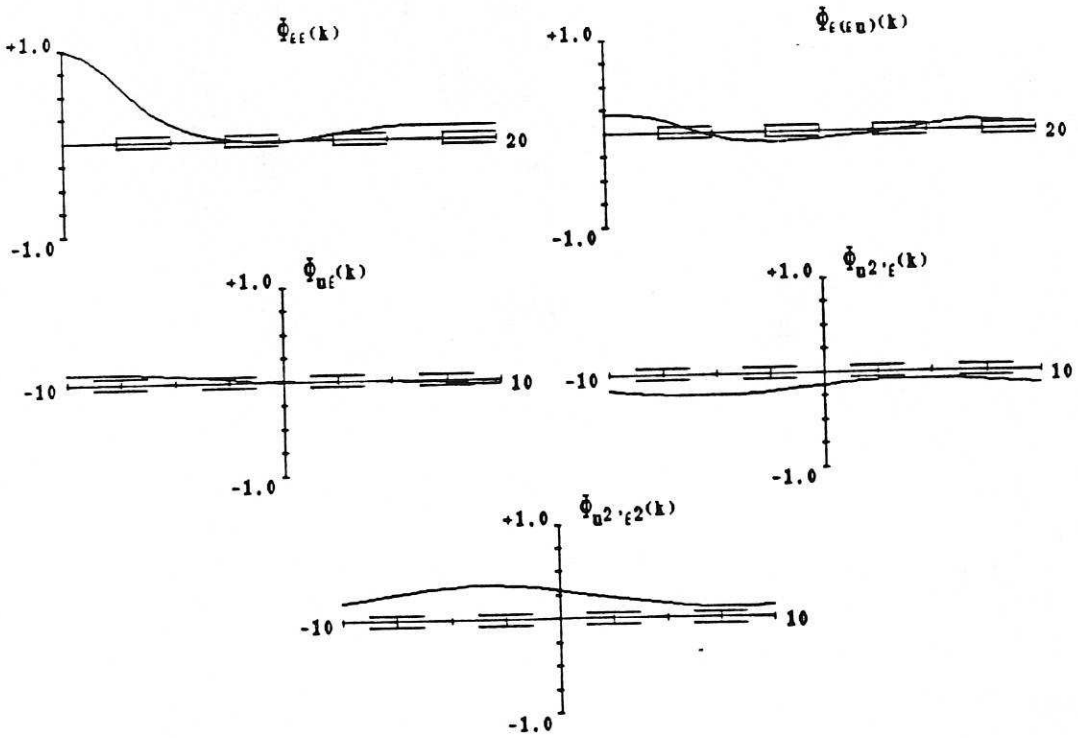
$\Phi_{\varepsilon\varepsilon}(k)$
$\Phi_{\varepsilon(\varepsilon u)}(k)$
$\Phi_{u\varepsilon}(k)$
$\Phi_{u^2\cdot\varepsilon}(k)$
$\Phi_{u^2\cdot\varepsilon^2}(k)$
+1.0
-1.0
20
10
-10

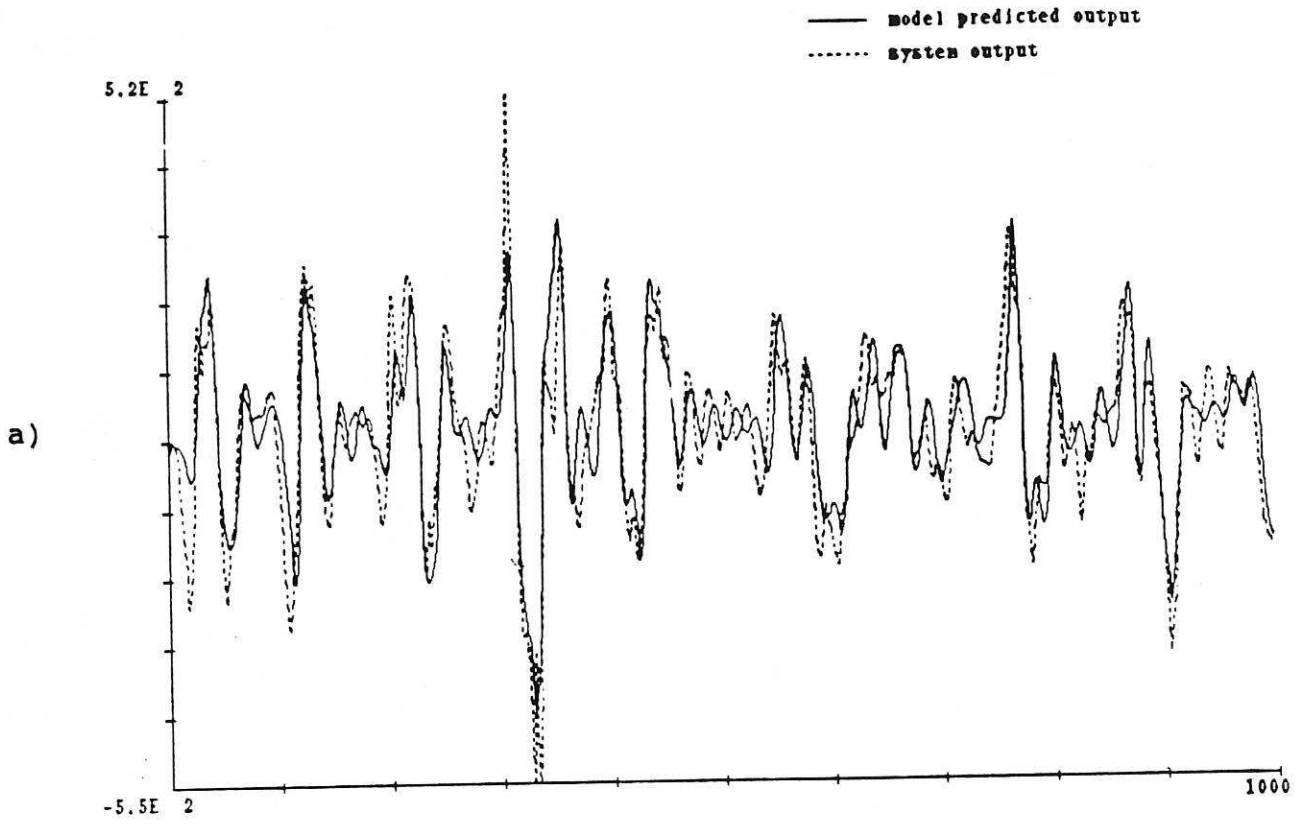
model predicted output
system output
5.2E 2
-5.5E 2
1000

a)

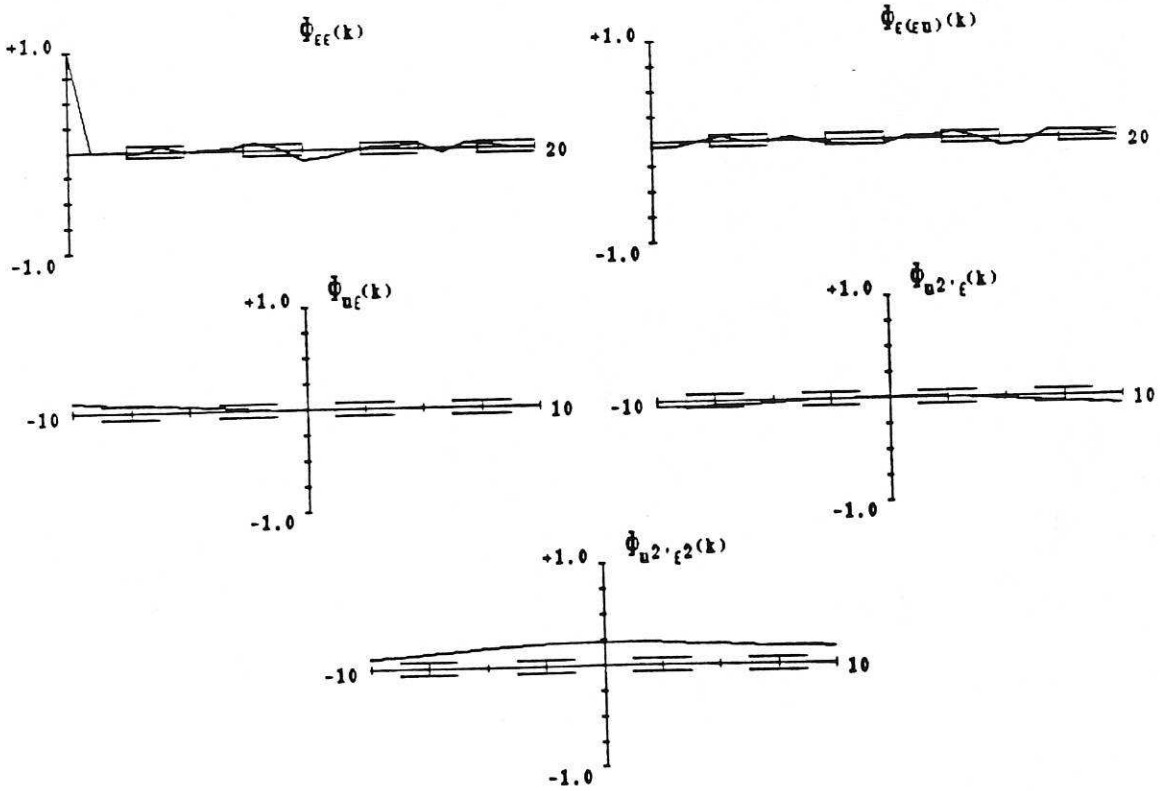
$\Phi_{\varepsilon\varepsilon}(k)$
$\Phi_{\varepsilon(\varepsilon u)}(k)$
$\Phi_{u\varepsilon}(k)$
$\Phi_{u2\cdot\varepsilon}(k)$
$\Phi_{u2\cdot\varepsilon 2}(k)$
+1.0
-1.0
20
10
-10

b)

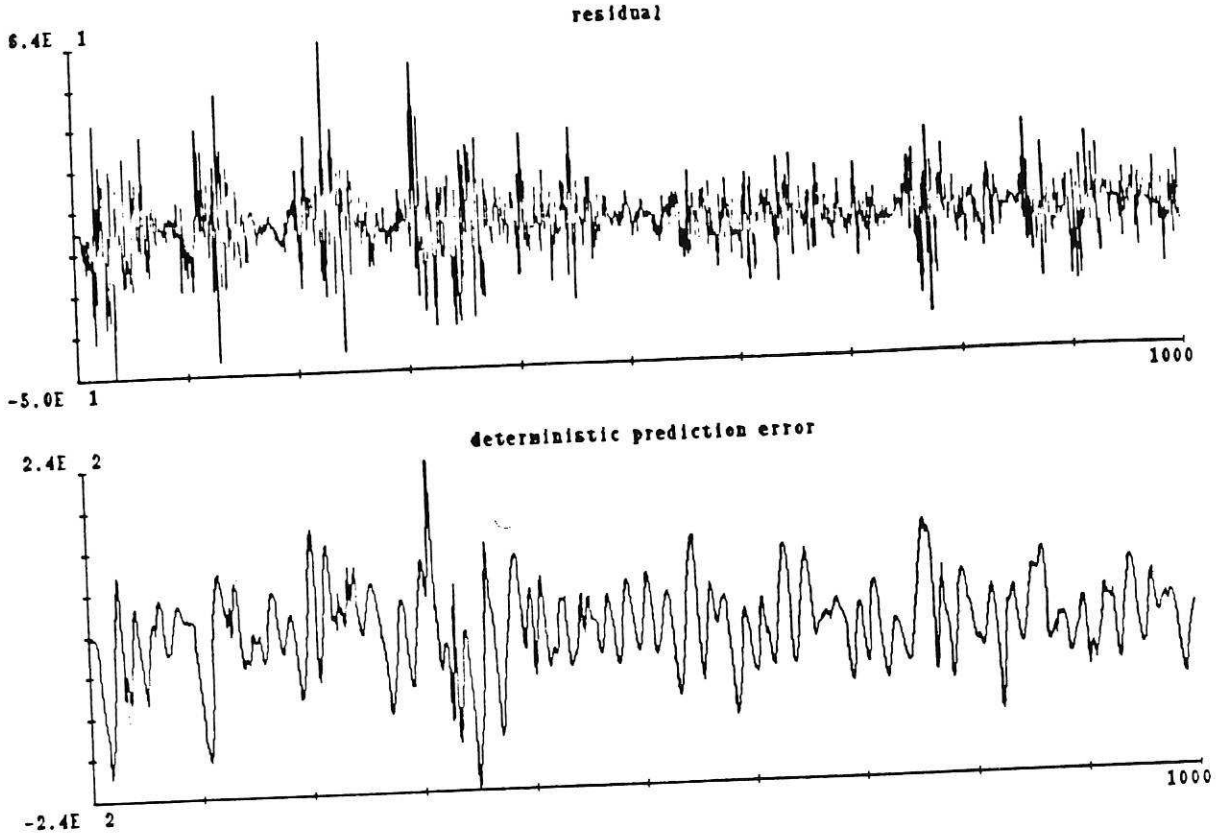
residual
6.4E 1
1000
-5.0E 1
deterministic prediction error
2.4E 2
1000
-2.4E 2